QCD phase diagram at high baryon densities

Wei-jie Fu

Dalian University of Technology

HENPIC Online Seminar, July 24, 2025

Based on:
WF, Xiaofeng Luo, Jan M. Pawlowski, Fabian Rennecke, Shi Yin, *PRD* 111 (2025) L031502, arXiv: 2308.15508;
Yang-yang Tan, Yong-rui Chen, WF, Wei-Jia Li, *Nature Commun.* 16 (2025) 2916, arXiv:2403.03503;
Hao-Lei Chen, WF, Xu-Guang Huang, Guo-Liang Ma, *PRL* 135 (2025) 032302, arXiv:2410.20704;
Jinhui Chen, WF, Shi Yin, Chunjian Zhang, arXiv:2504.06886;
Zi-ning Wang, Li-jun Zhou, Chuang Huang, WF, in preparation;
Rui-zhe Zhao, Shi Yin, WF, in preparation;
Yang-yang Tan, Shi Yin, Yong-rui Chen, Chuang Huang, WF, in preparation.

CEP in QCD phase diagram

QCD phase diagram

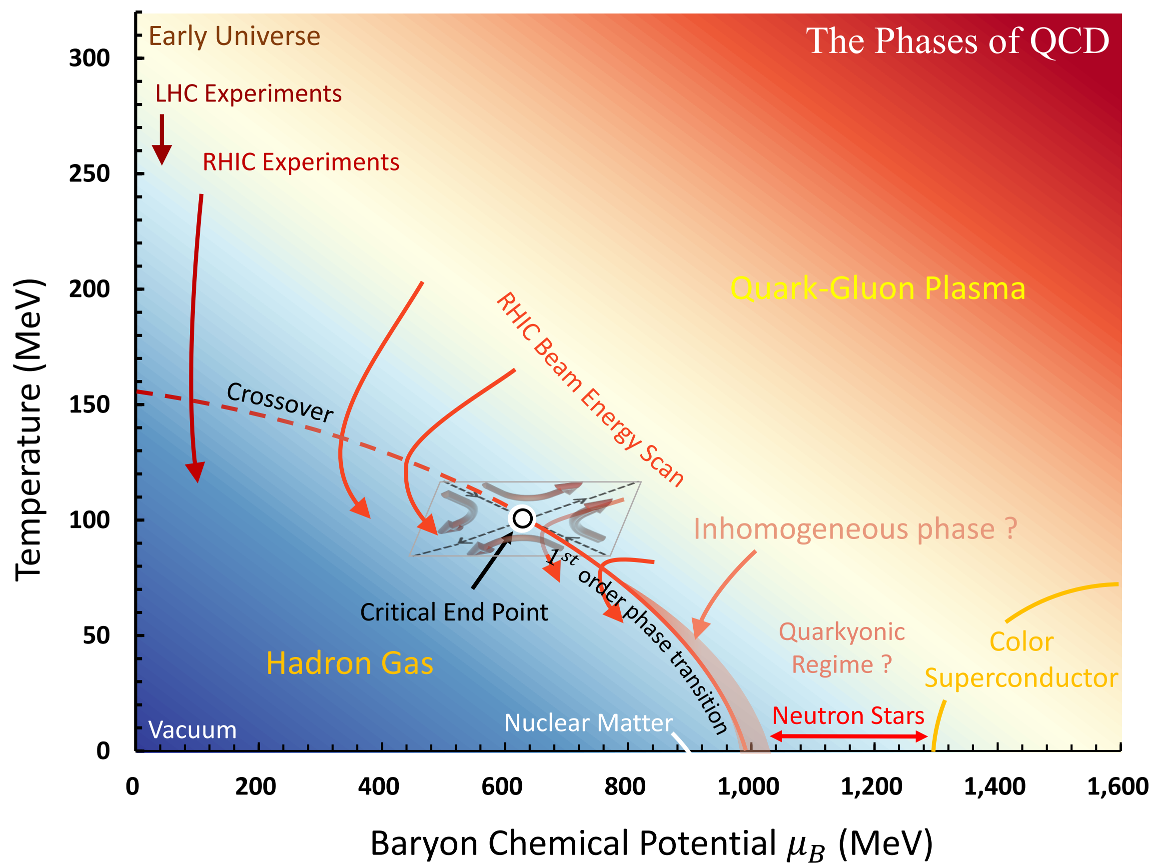

Non-monotonicity:
M. Stephanov, *PRL* 107 (2011) 052301

Fluctuations measured in BES-II

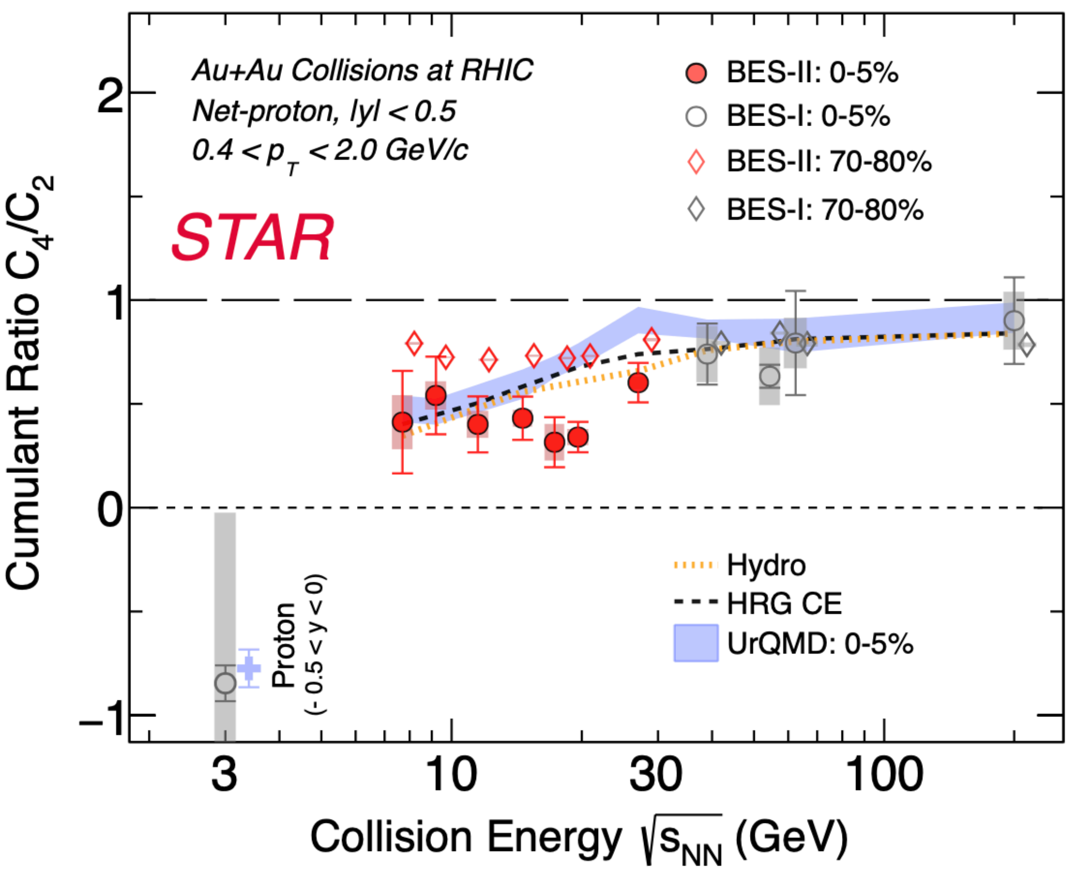

Ashish Pandav for STAR Collaboration in CPOD2024

STAR Collaboration, arXiv:2504.00817

- Is there a "peak" structure serving as the smoking gun signal for the critical end point in the QCD phase diagram?

CEP in QCD phase diagram

QCD phase diagram

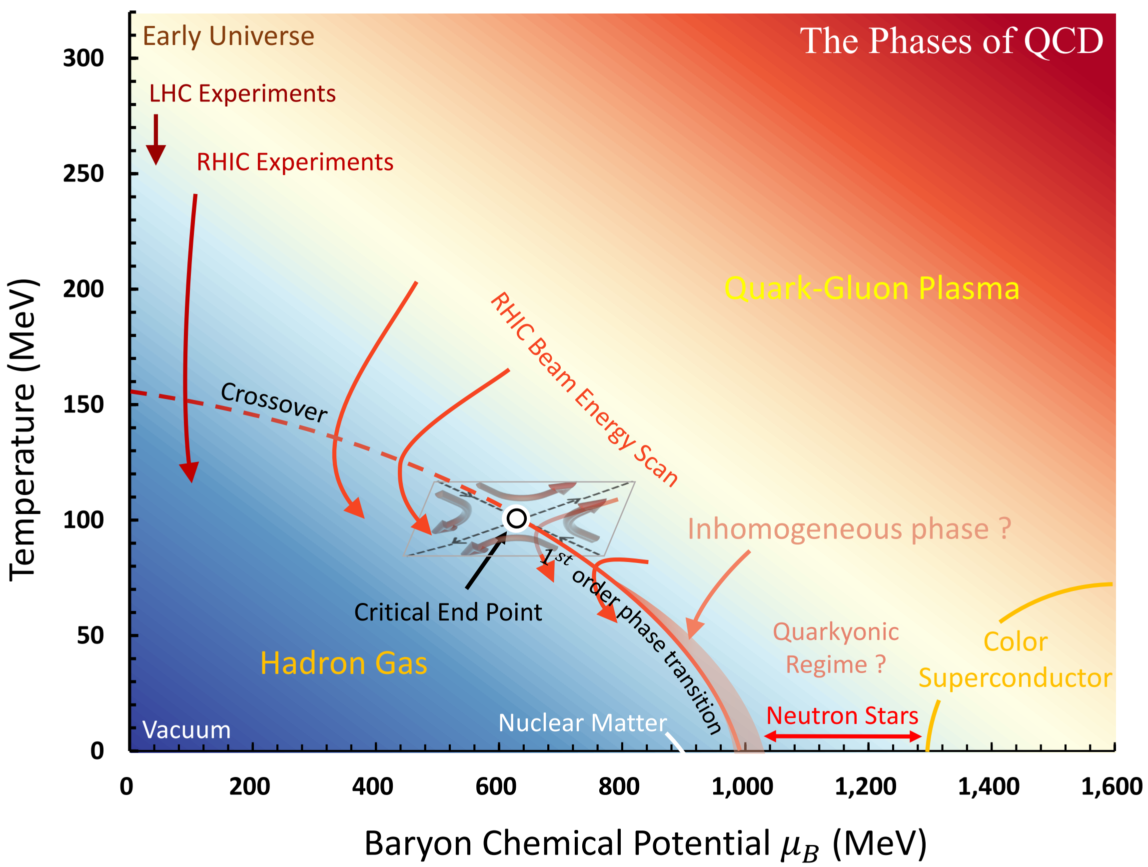

Non-monotonicity:
M. Stephanov, *PRL* 107 (2011) 052301

Fluctuations measured in BES-II

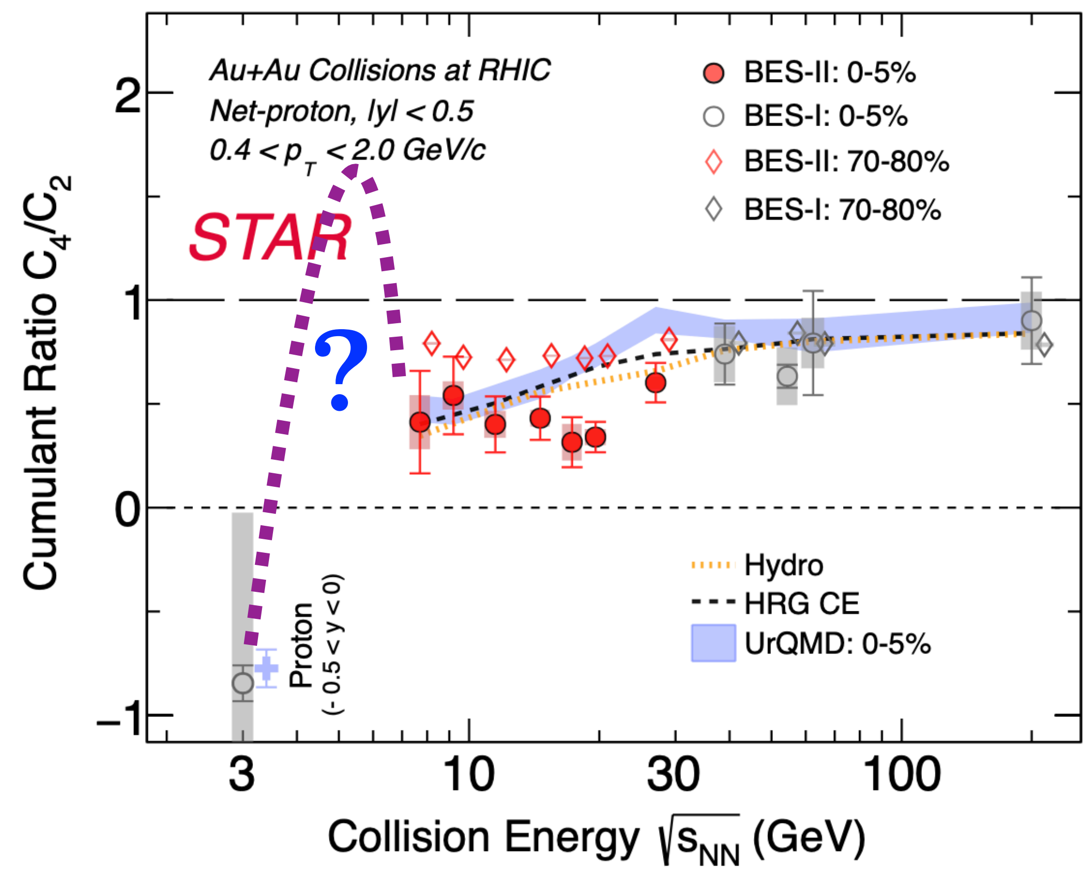

Ashish Pandav for STAR Collaboration in CPOD2024

STAR Collaboration, arXiv:2504.00817

- Is there a "peak" structure serving as the smoking gun signal for the critical end point in the QCD phase diagram?

Critical slowing down near QCD critical point

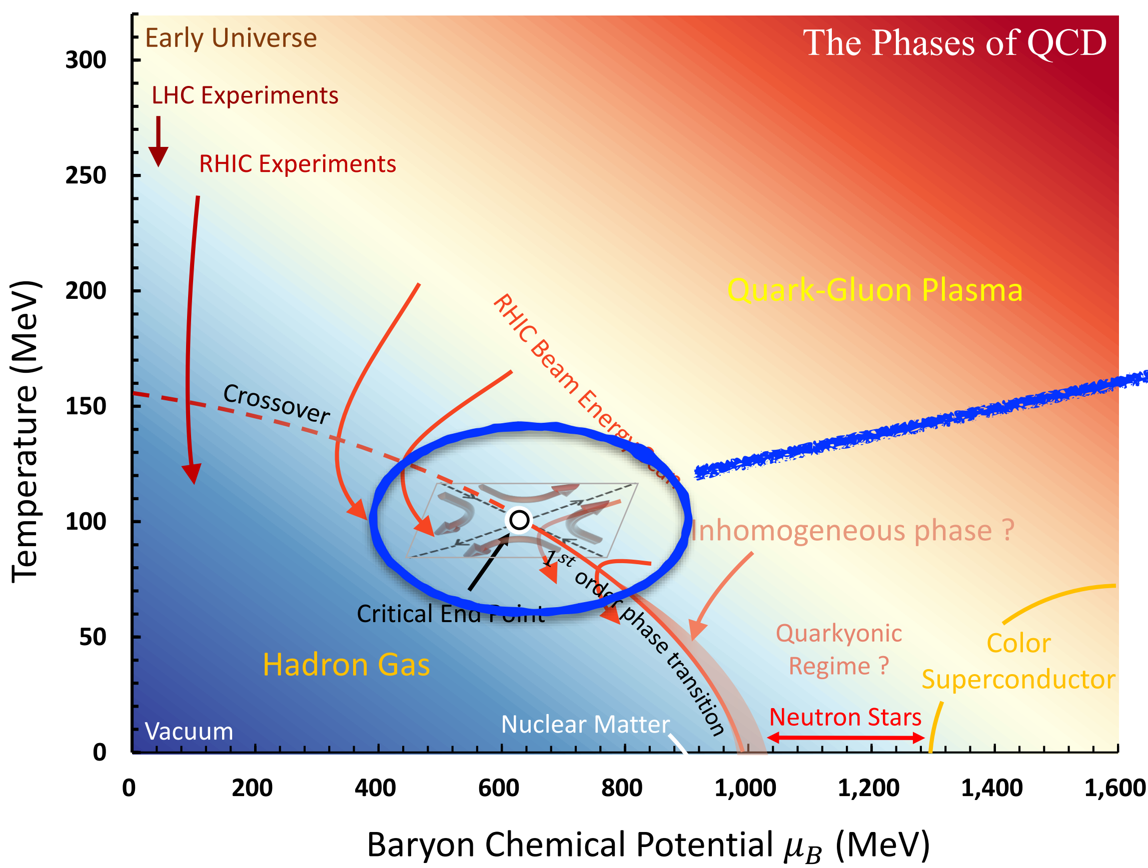

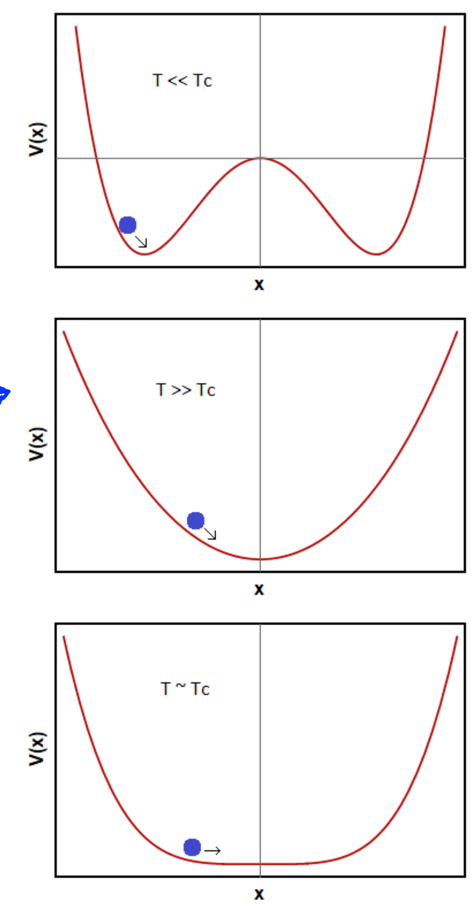

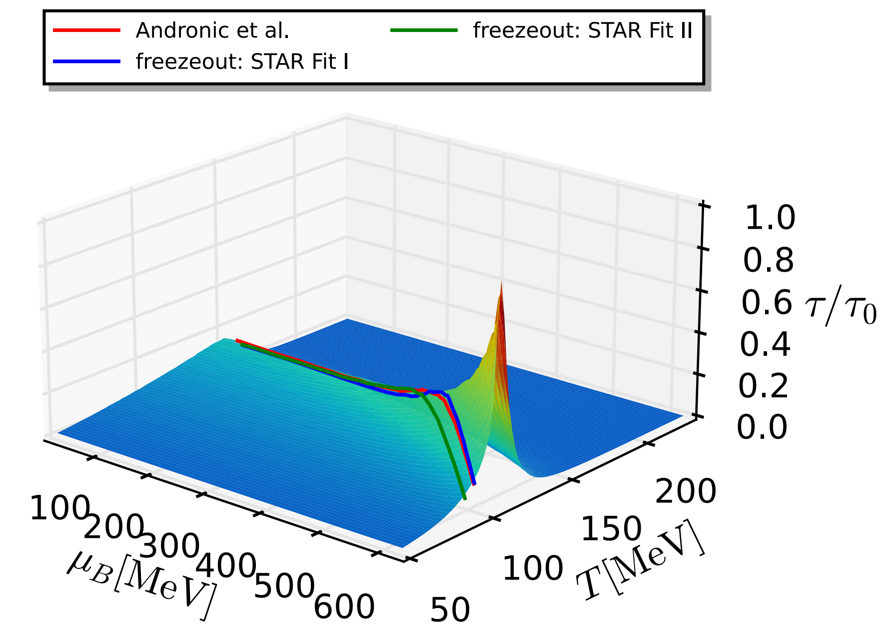

Tan, Yin, Chen, Huang, WF, in preparation

Relaxation time:

$$\tau = \xi^z f(k\xi)$$

z: **dynamic critical exponent**

Goldstone damping

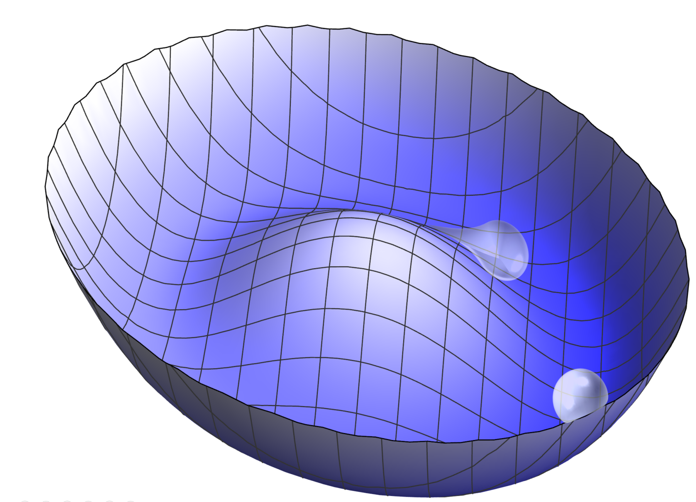

Call for:

- Real-time description of strongly interacting systems.
- Nonperturbative approach of QCD.

Outline

- Introduction
- Recent estimate of location of CEP
- Baryon number fluctuations
- Spin fluctuations and correlations
- Temperature fluctuations
- Real-time dynamics near phase transitions
- Summary and outlook

First-principles QCD within fRG

QCD flow equation:

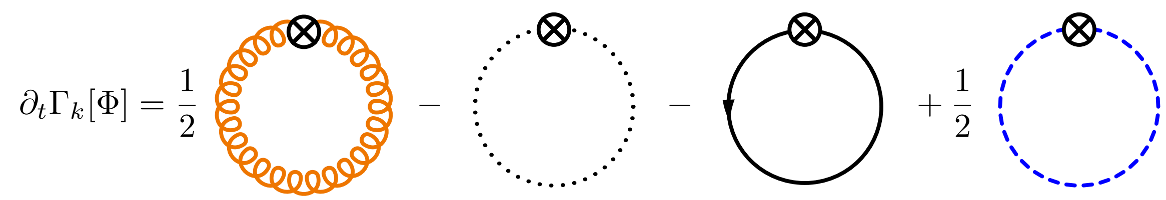

Glue sector:

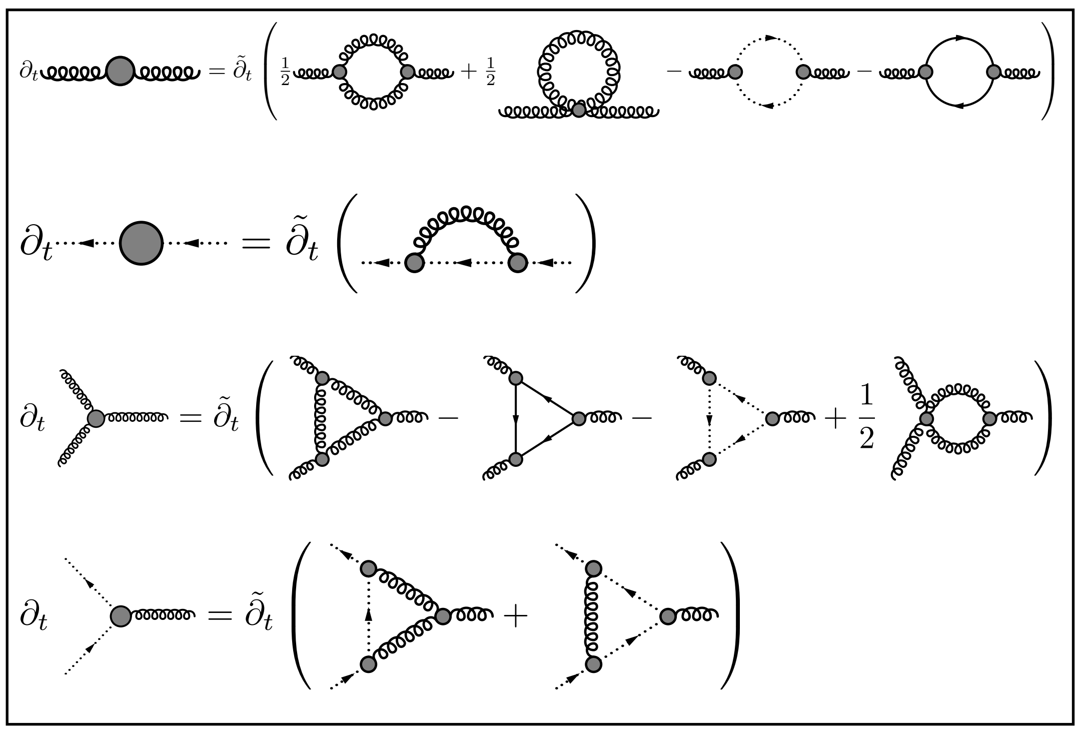

Matter sector:

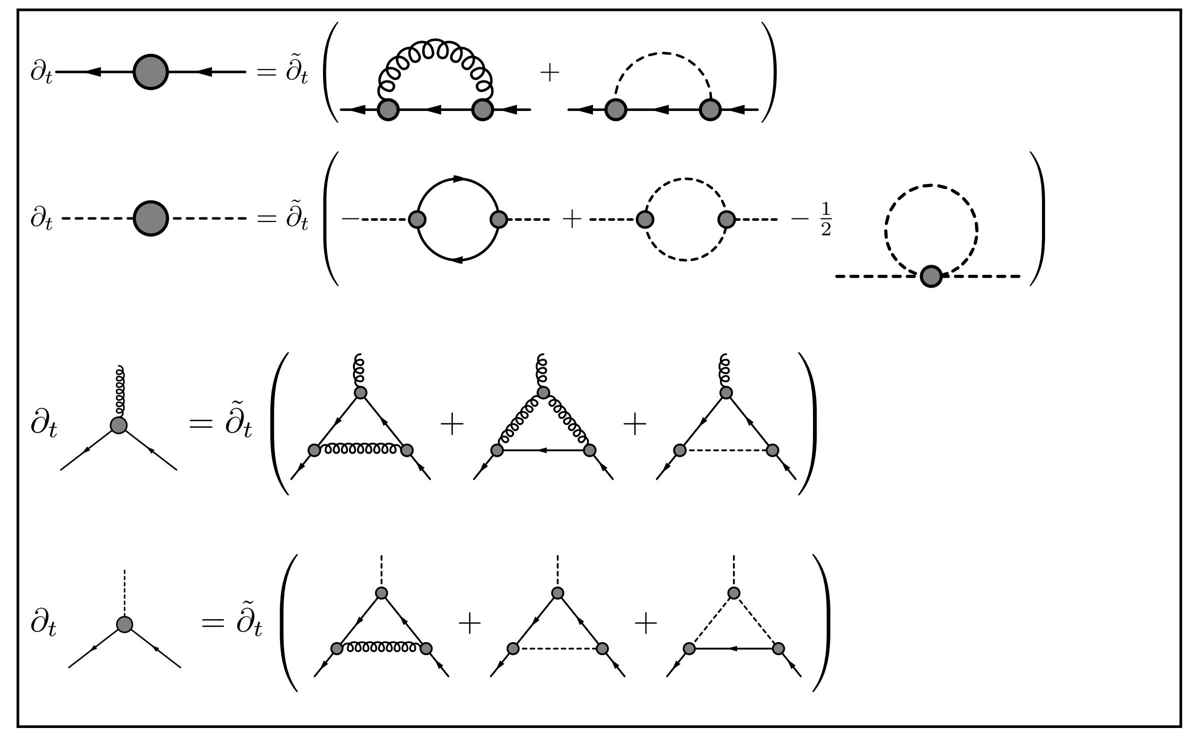

quark condensate:

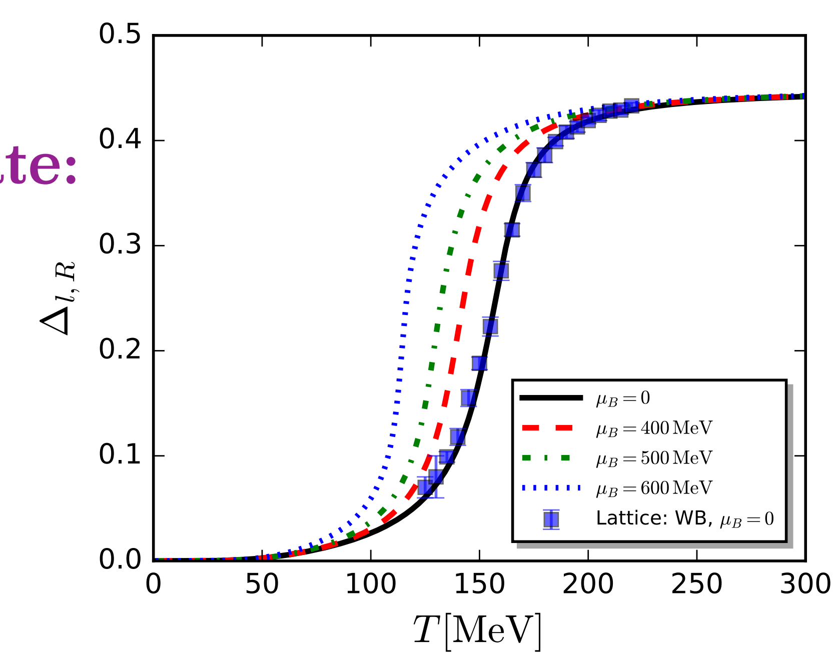

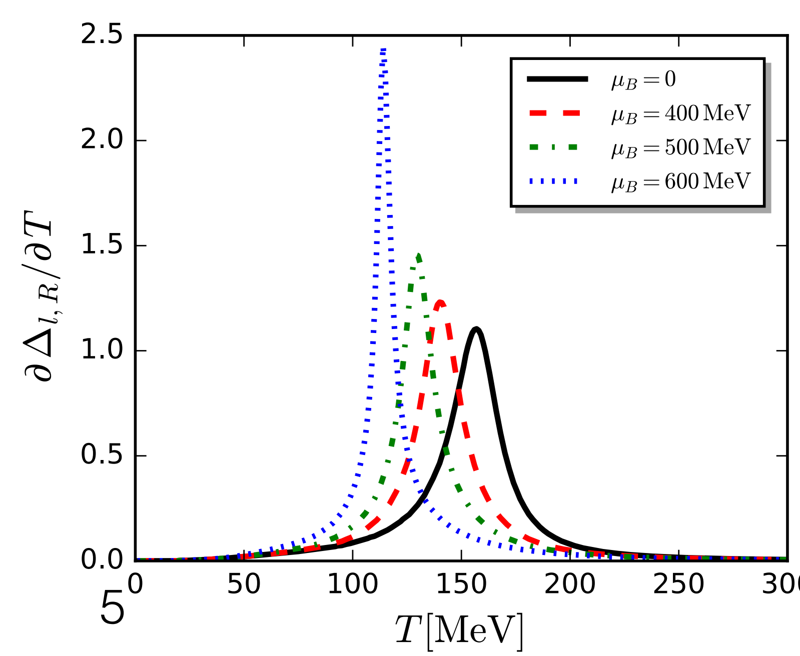

fRG:WF, Pawlowski, Rennecke, *PRD* 101 (2020) 054032

Lattice: Borsanyi *et al.* (WB), *JHEP* 09 (2010) 073

Quantitative errors analysis in fRG: Ihssen, Pawlowski, Sattler, Wink, arXiv:2408.08413

CEP from different theoretical calculations

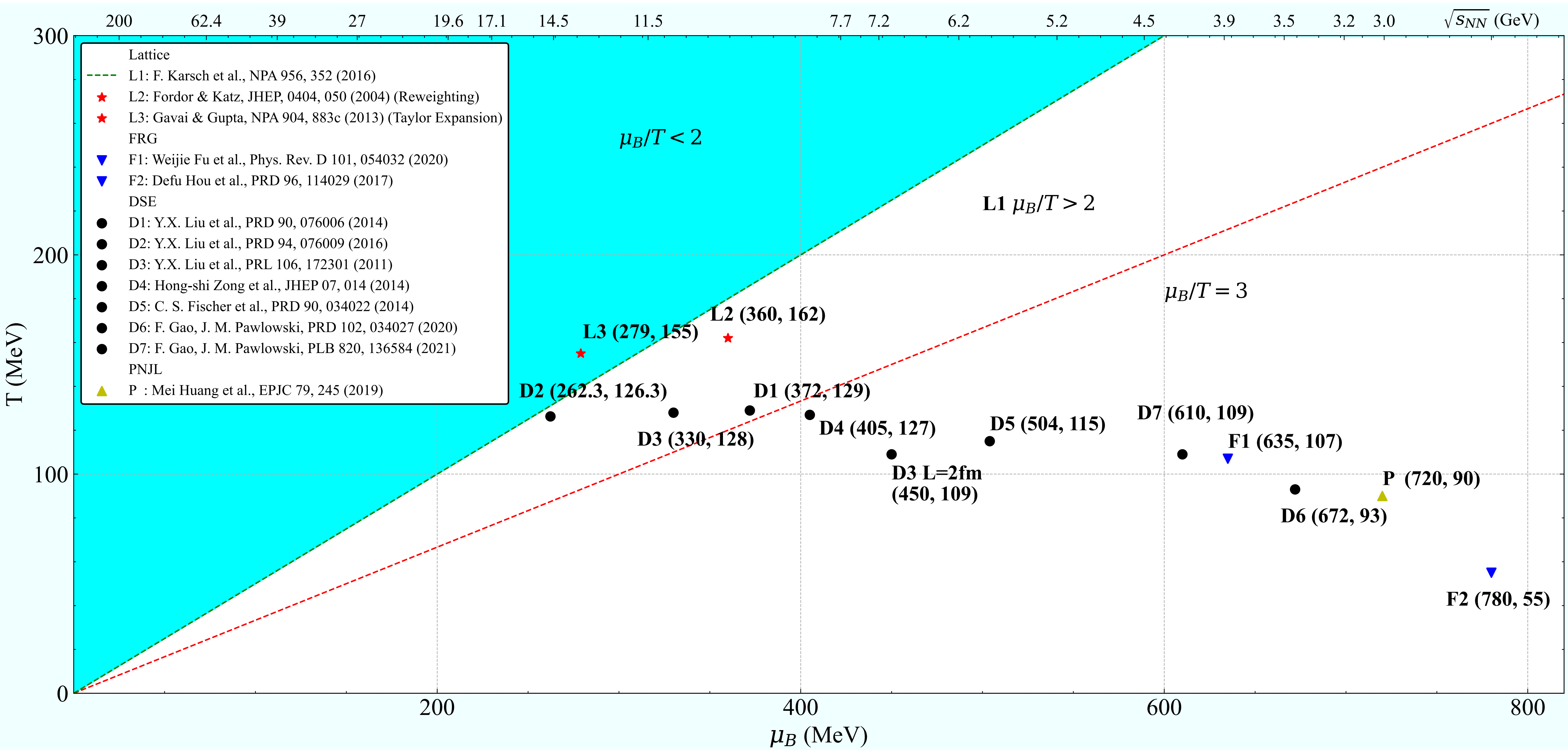

By courtesy of Xiaofeng Luo

CEP from first-principles functional QCD

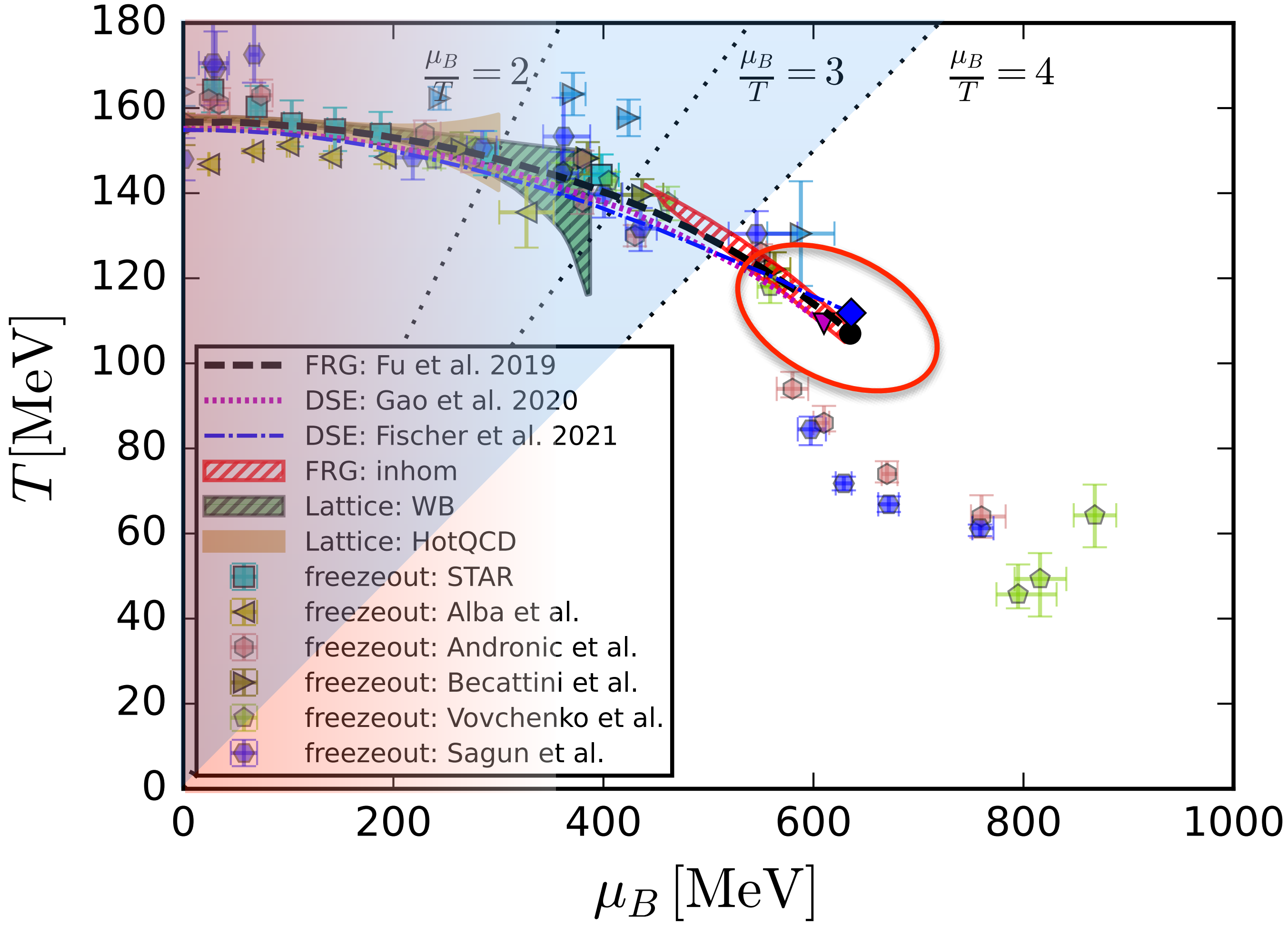

Passing through strict benchmark tests in comparison to lattice QCD at vanishing and small μ_B.

Regime of quantitative reliability of functional QCD with $\mu_B/T \lesssim 4$.

Estimates of the location of CEP from first-principles functional QCD:

fRG:

● $(T,\mu_B)_{\mathrm{CEP}} = (107, 635)\mathbf{MeV}$

fRG: WF, Pawlowski, Rennecke, *PRD* 101 (2020), 054032

DSE:

▼ $(T,\mu_B)_{\mathrm{CEP}} = (109, 610)\mathbf{MeV}$

DSE (fRG): Gao, Pawlowski, *PLB* 820 (2021) 136584

◆ $(T,\mu_B)_{\mathrm{CEP}} = (112, 636)\mathbf{MeV}$

DSE: Gunkel, Fischer, *PRD* 104 (2021) 5, 054022

- No CEP observed in $\mu_B/T \lesssim 2 \sim 3$ from lattice QCD. Karsch, *PoS* CORFU2018 (2019)163
- Recent studies of QCD phase structure from both fRG and DSE have shown convergent estimate for the location of CEP: 600 MeV $\lesssim \mu_{B_{\mathrm{CEP}}} \lesssim$ 650 MeV.

CEP from other approaches

Recent estimates of the location of CEP:

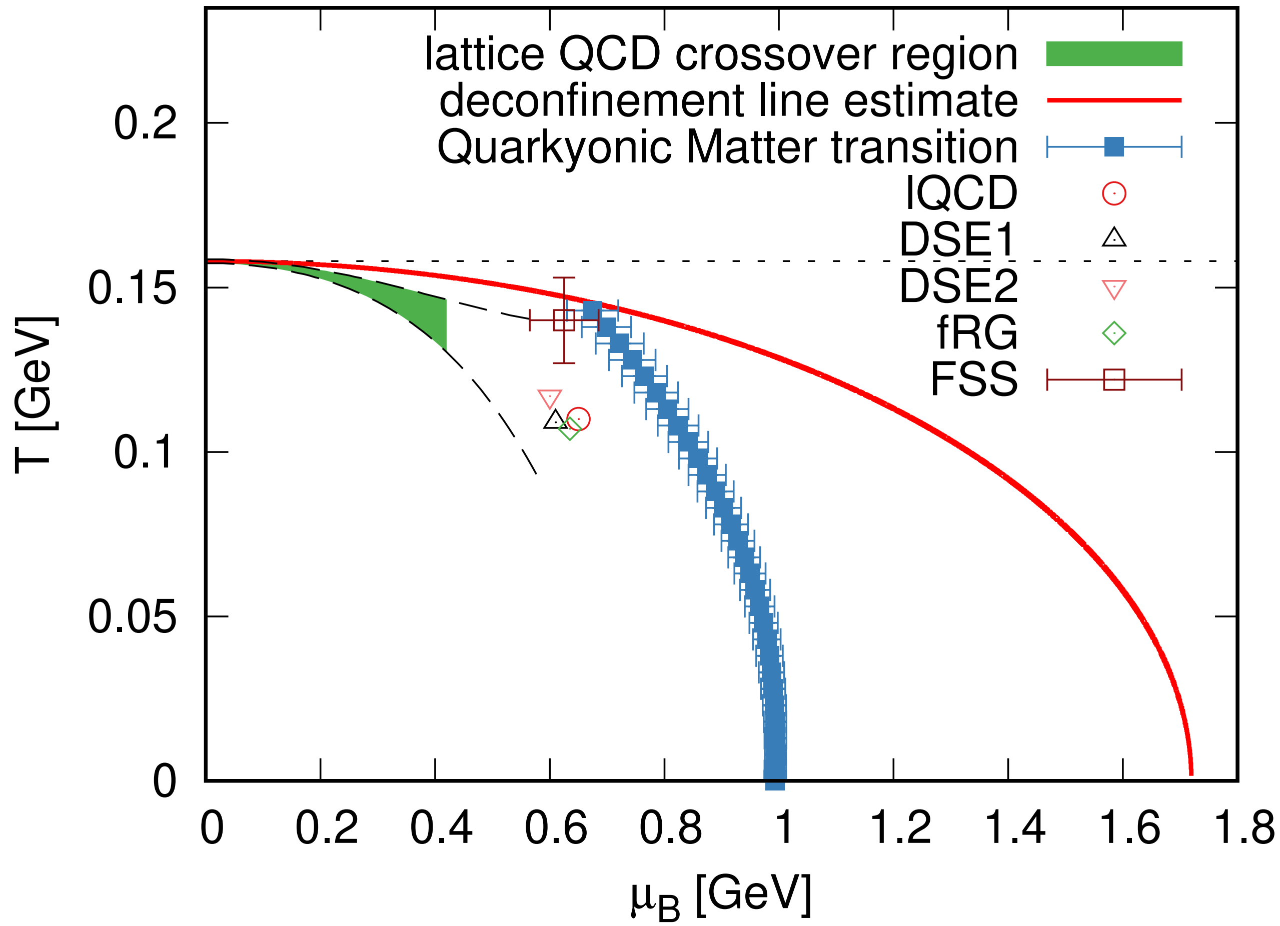

Figure from:
Bluhm, Fujimoto, McLerran, Nahrgang, *PRC* 111 (2025) 044914, arXiv:2409.12088

fRG:
WF, Pawlowski, Rennecke, *PRD* 101 (2020), 054032, arXiv:1909.02991.
DSE1:
Gao, Pawlowski, *PLB* 820 (2021) 136584, arXiv:2010.13705.
DSE2:
Gunkel, Fischer, *PRD* 104 (2021) 054022, arXiv:2106.08356.
Lattice extrapolation (Yang-Lee edge singularities):
David A. Clarke *et al.*, arXiv:2405.10196.
Finite-size-scaling analysis:
A. Sorensen, P. Sorensen, arXiv:2405.10278.

- **Estimates of the location of CEP in the QCD phase diagram have arrived at convergence from different approaches.**

CEP from other approaches

Recent estimates of the location of CEP:

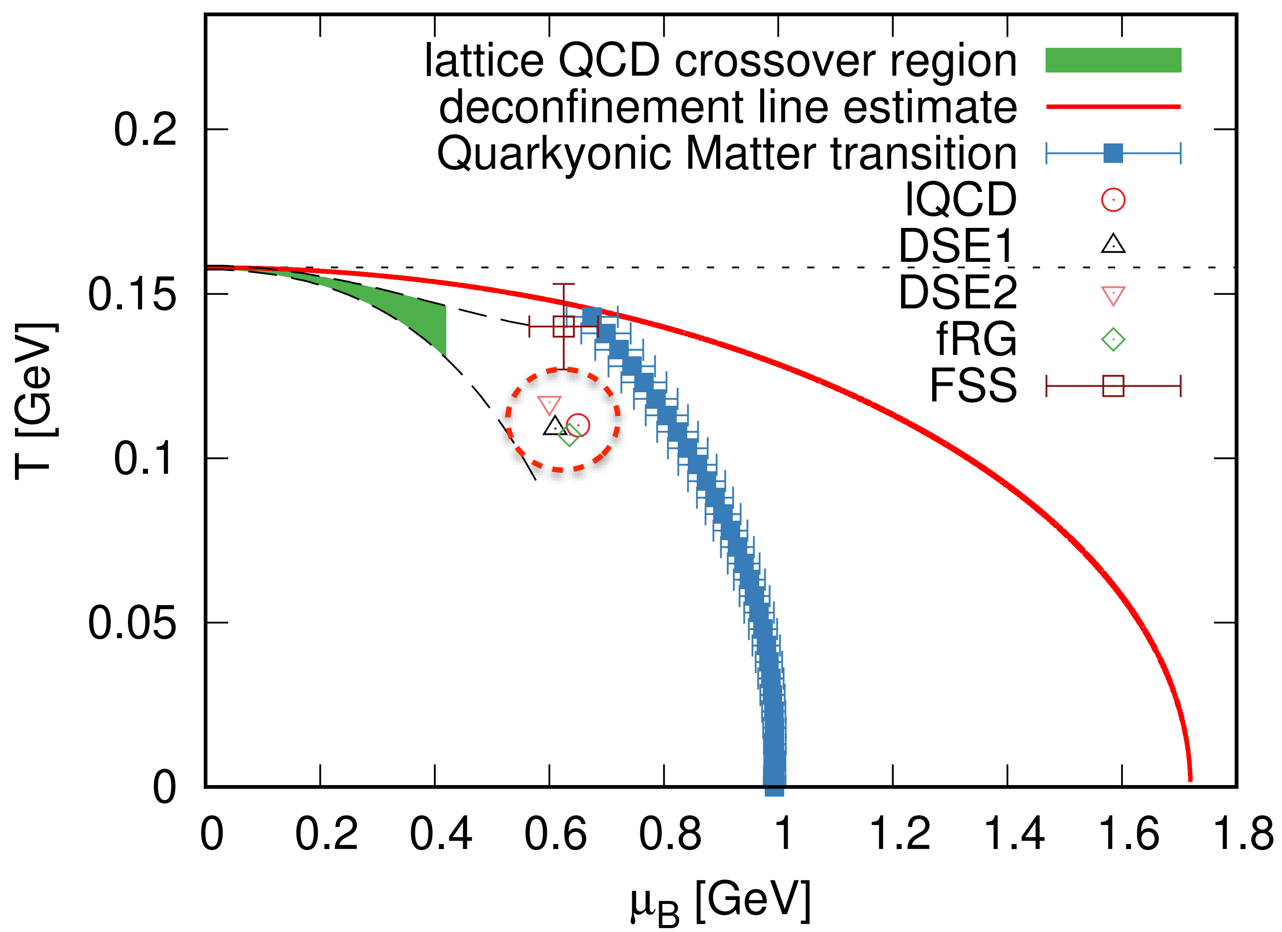

Figure from:
Bluhm, Fujimoto, McLerran, Nahrgang, *PRC* 111 (2025) 044914, arXiv:2409.12088

fRG:
WF, Pawlowski, Rennecke, *PRD* 101 (2020), 054032, arXiv:1909.02991.
DSE1:
Gao, Pawlowski, *PLB* 820 (2021) 136584, arXiv:2010.13705.
DSE2:
Gunkel, Fischer, *PRD* 104 (2021) 054022, arXiv:2106.08356.
Lattice extrapolation (Yang-Lee edge singularities):
David A. Clarke *et al.*, arXiv:2405.10196.
Finite-size-scaling analysis:
A. Sorensen, P. Sorensen, arXiv:2405.10278.

- **Estimates of the location of CEP in the QCD phase diagram have arrived at convergence from different approaches.**

QCD phase diagram obtained from Fierz-complete four-quark basis

Updated QCD phase diagram:

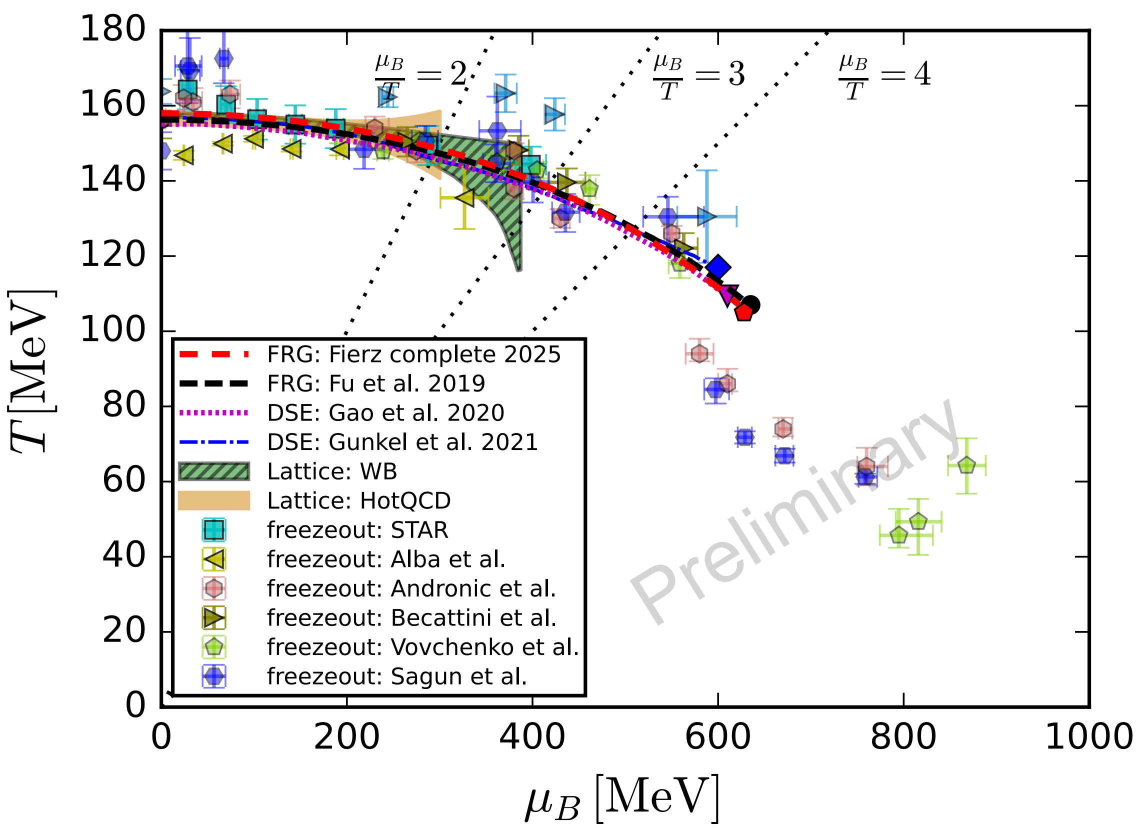

Four-quark couplings:

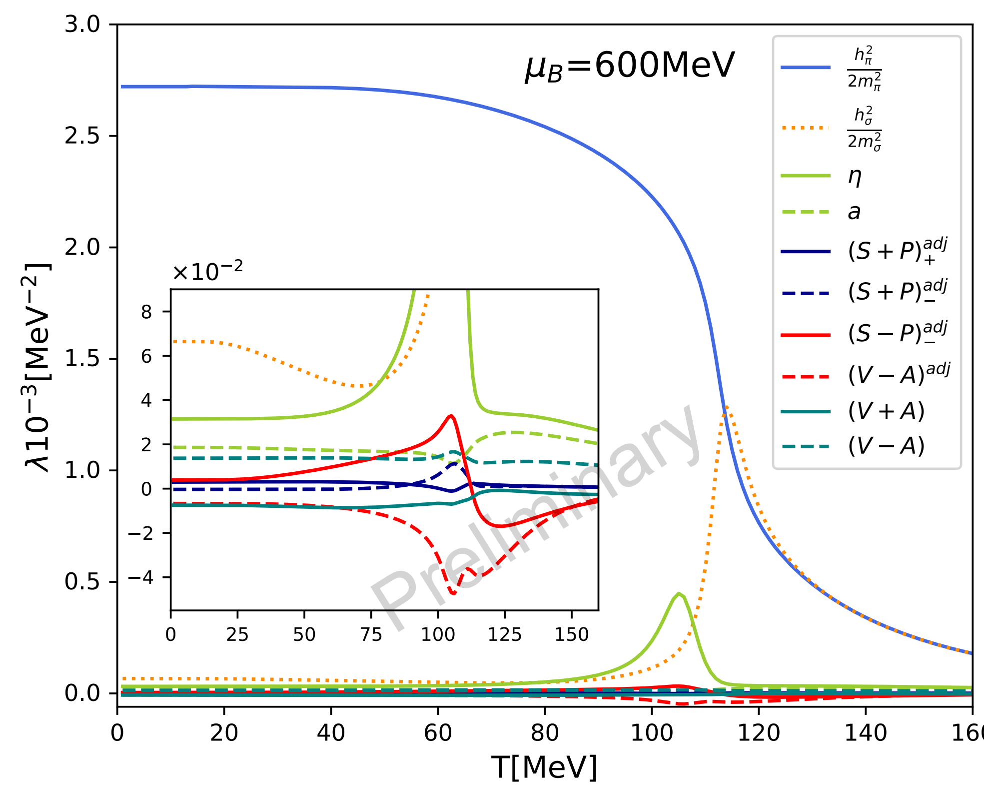

Scalar-pseudoscalar channel:

$$(T,\mu_B)_{\mathrm{CEP}} = (107, 635)\ \mathbf{MeV}$$

Fierz-complete channels:

$$(T,\mu_B)_{\mathrm{CEP}} = (105, 630)\ \mathbf{MeV}$$

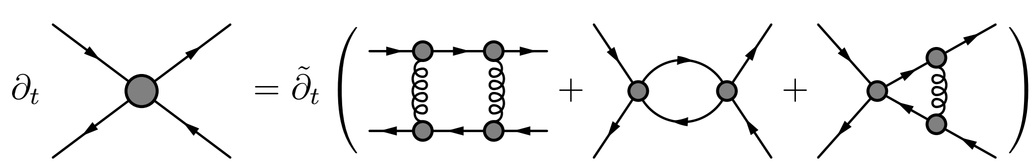

Zi-ning Wang, Li-jun Zhou, Chuang Huang, WF, in preparation

Baryon number fluctuations

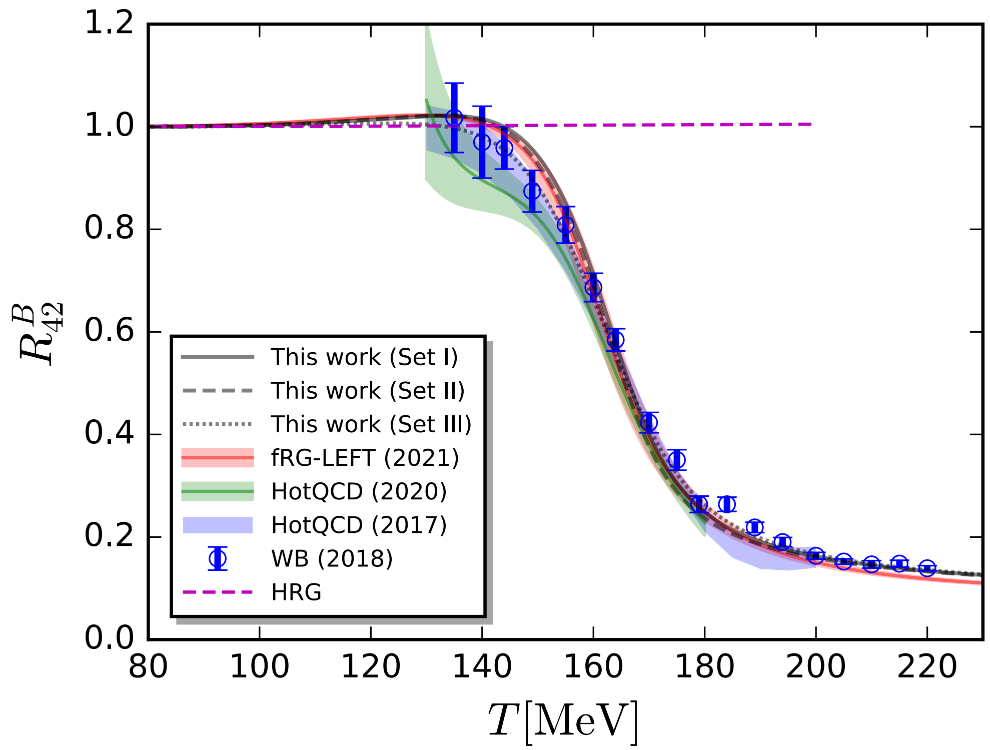

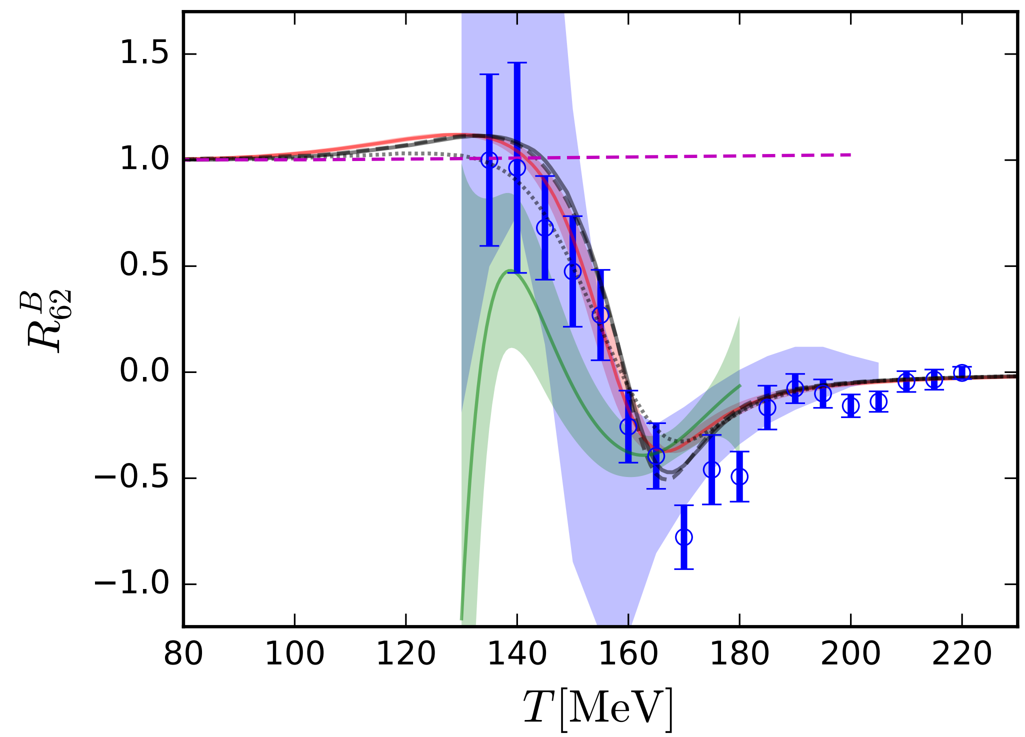

$\mu_B = 0$

fRG: WF, Luo, Pawlowski, Rennecke, Yin, *PRD* 111 (2025) L031502, arXiv: 2308.15508; WF, Luo, Pawlowski, Rennecke, Wen, Yin, *PRD* 104 (2021) 094047

HotQCD: A. Bazavov *et al.*, arXiv: *PRD* 95 (2017), 054504; *PRD* 101 (2020), 074502

WB: S. Borsanyi *et al.*, arXiv: *JHEP* 10 (2018) 205

baryon number fluctuations

$$\chi_n^B = \frac{\partial^n}{\partial(\mu_B/T)^n}\frac{p}{T^4} \qquad R_{nm}^B = \frac{\chi_n^B}{\chi_m^B}$$

relation to the cumulants

$$\frac{M}{VT^3} = \chi_1^B\,,\ \frac{\sigma^2}{VT^3} = \chi_2^B\,,\ S = \frac{\chi_3^B}{\chi_2^B\sigma}\,,\ \kappa = \frac{\chi_4^B}{\chi_2^B\sigma^2}\,,$$

- **In comparison to lattice results and our former results, the improved results of baryon number fluctuations at vanishing chemical potential in the QCD-assisted LEFT are convergent and consistent.**

Canonical fluctuations at the freeze-out

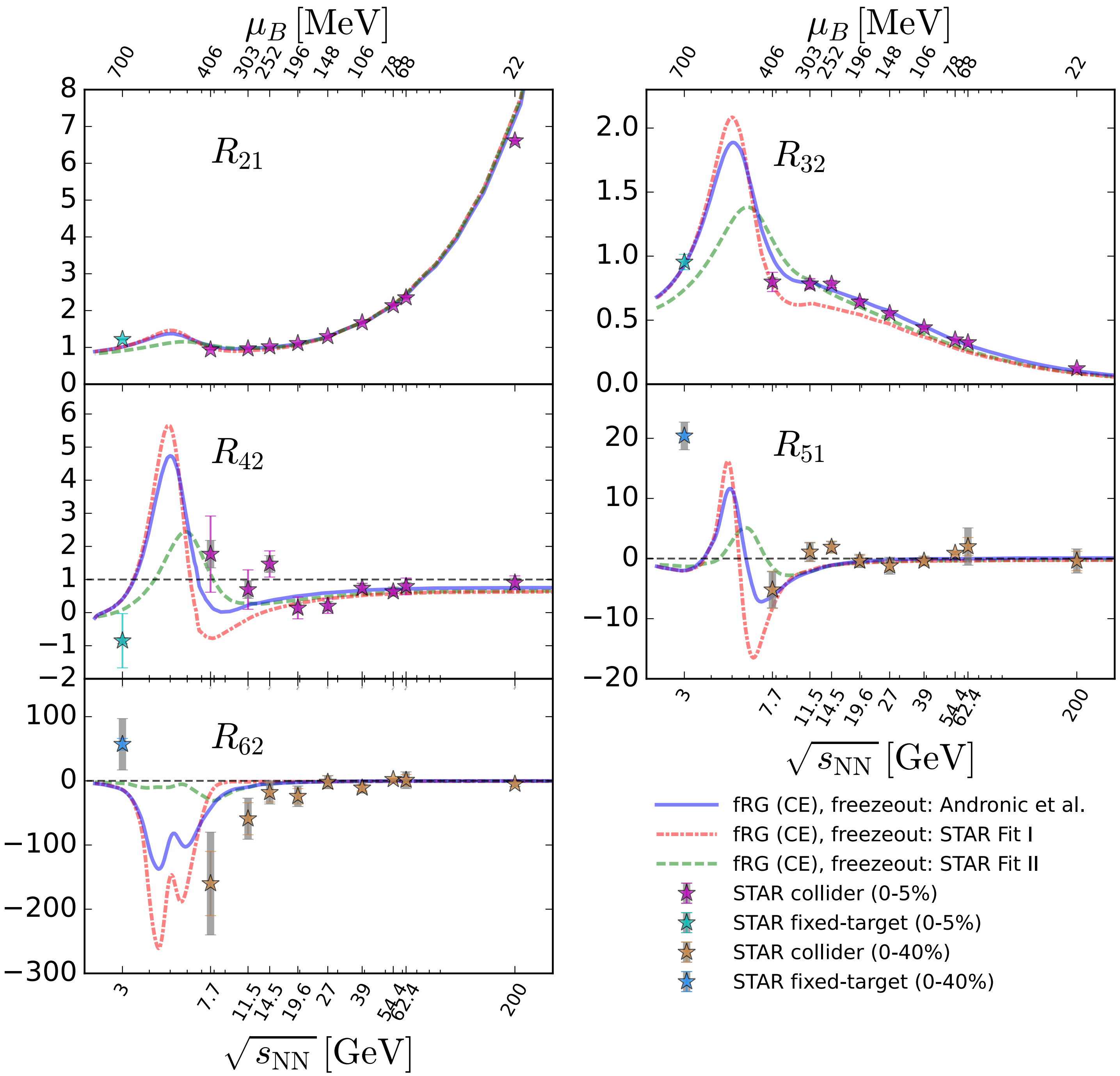

STAR: Adam *et al.* (STAR), *PRL* 126 (2021) 092301; Abdallah *et al.* (STAR), *PRL* 128 (2022) 202303; Aboona *et al.* (STAR), *PRL* 130 (2023) 082301

fRG: WF, Luo, Pawlowski, Rennecke, Yin, *PRD* 111 (2025) L031502, arXiv: 2308.15508

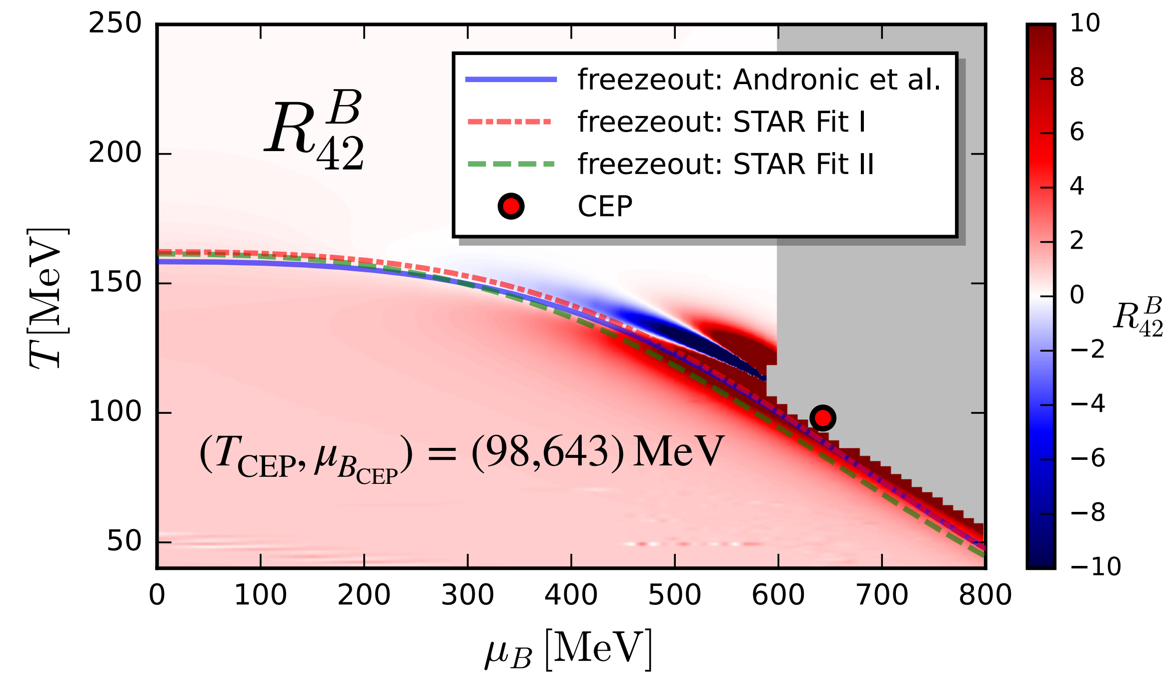

- **Peak structure is found in 3 GeV $\lesssim \sqrt{s_{\mathrm{NN}}} \lesssim$ 7.7 GeV.**
- **Position of peak in R_{42} is $\mu_{B_{\mathrm{peak}}} =$ 536, 541 and 486 MeV for the three freeze-out curves, significantly smaller than $\mu_{B_{\mathrm{CEP}}} = 643$ MeV.**

C_4/C_2: Comparison to STAR data

FXT energies at 3.2, 3.5, 3.9 GeV:

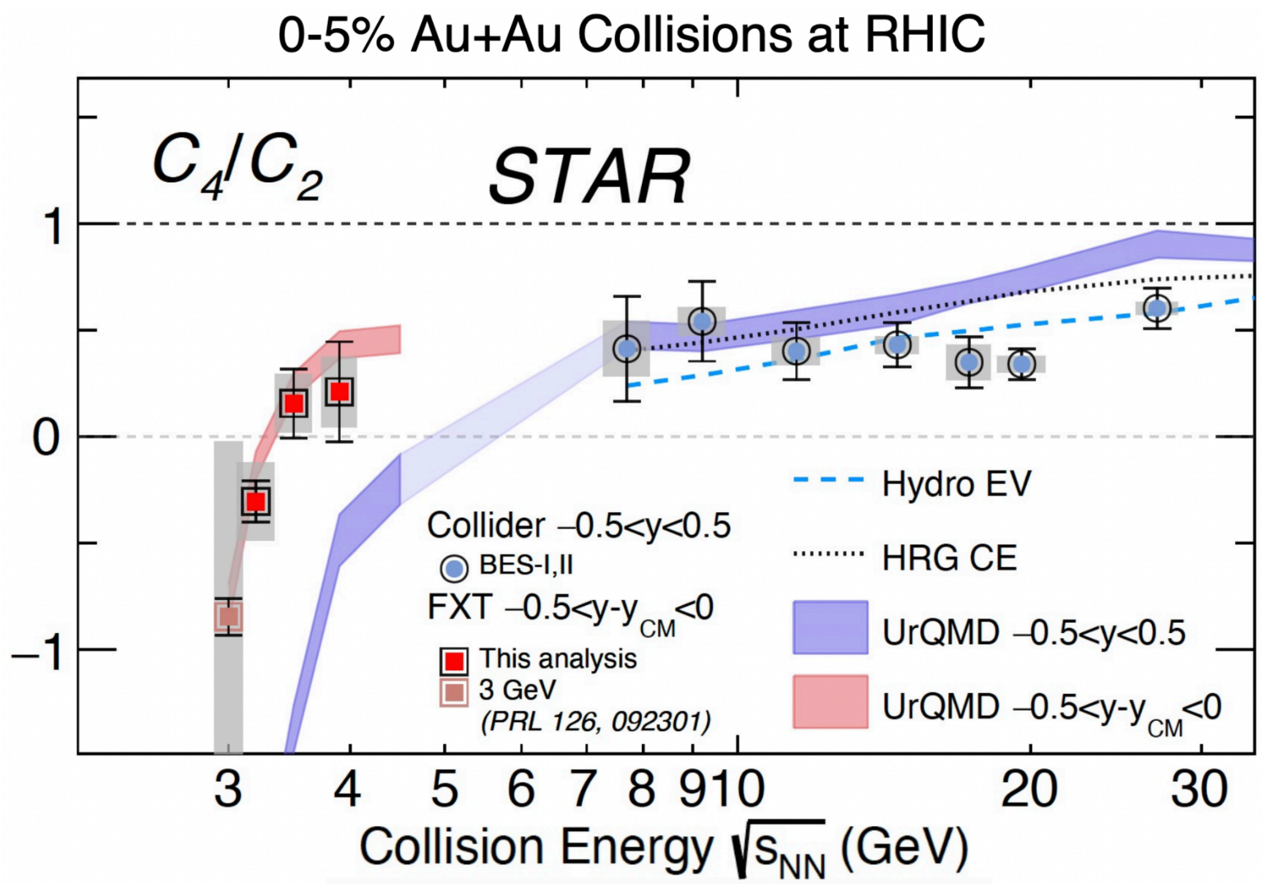

STAR: Z. Sweger, Quark Matter 2025
STAR: arXiv:2504.00817

Net baryon (proton) number kurtosis:

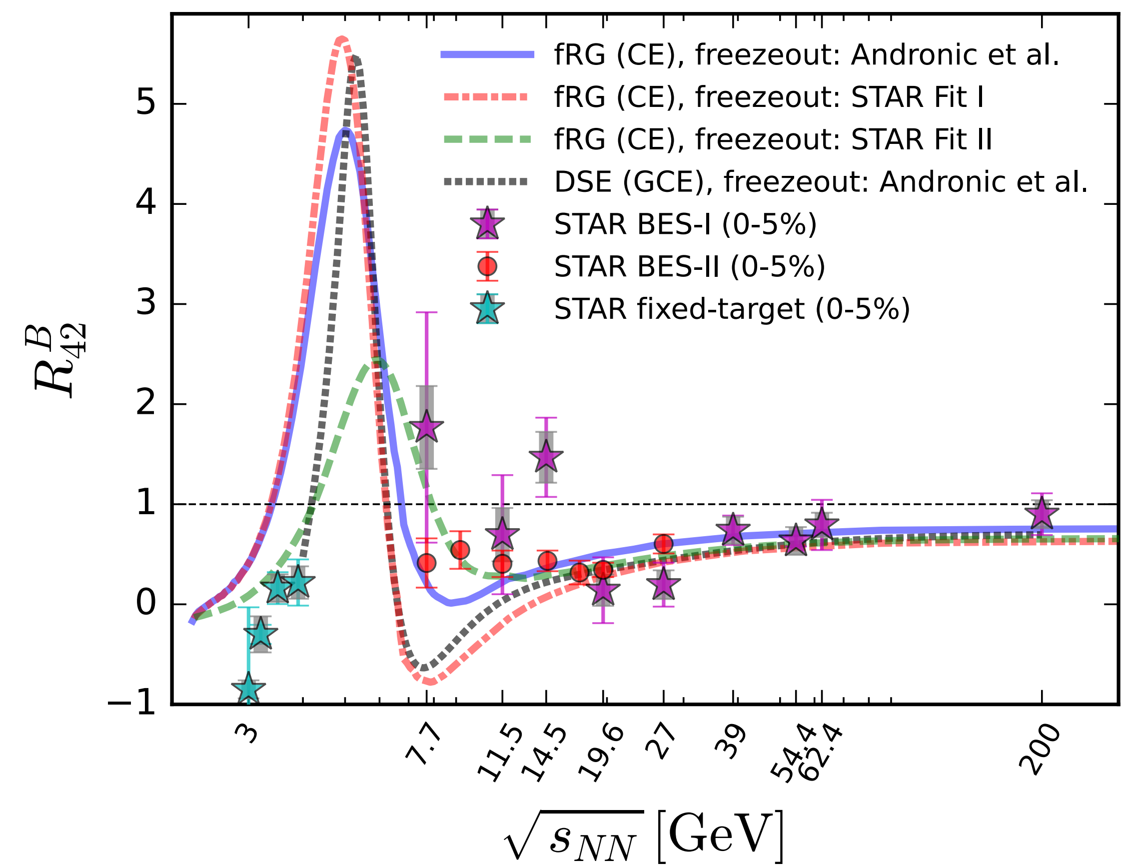

fRG: WF, Luo, Pawlowski, Rennecke, Yin, *PRD* 111 (2025) L031502, arXiv: 2308.15508
DSE: Lu, Gao, Liu, Pawlowski, arXiv: 2504.05099

- **Theoretical prediction with critical fluctuations (fRG and DSE) is consistent with STAR data.**
- **A peak structure is predicted in the energy regime of fixed-target experiments, i.e. 3 GeV $\lesssim \sqrt{s_{\rm NN}} \lesssim$ 7.7 GeV. Experimental search of this peak is very important.**

C_3/C_1: Comparison to STAR data

STAR data and UrQMD (baseline):

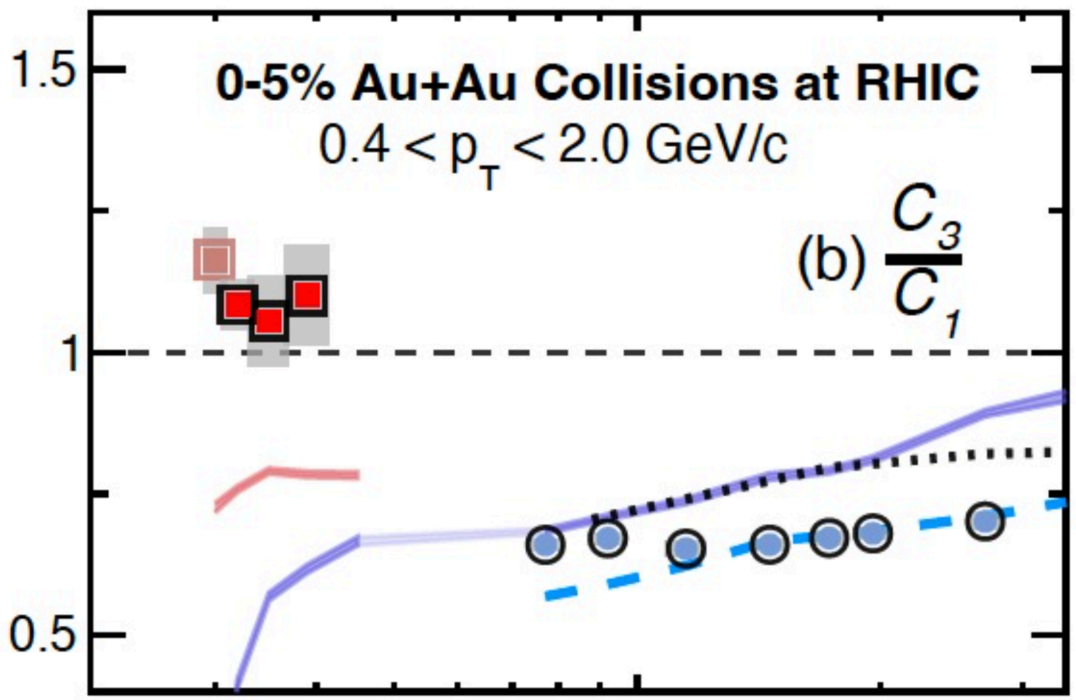

STAR: Z. Sweger, Quark Matter 2025
STAR: arXiv:2504.00817

fRG (critical) and HRG (baseline):

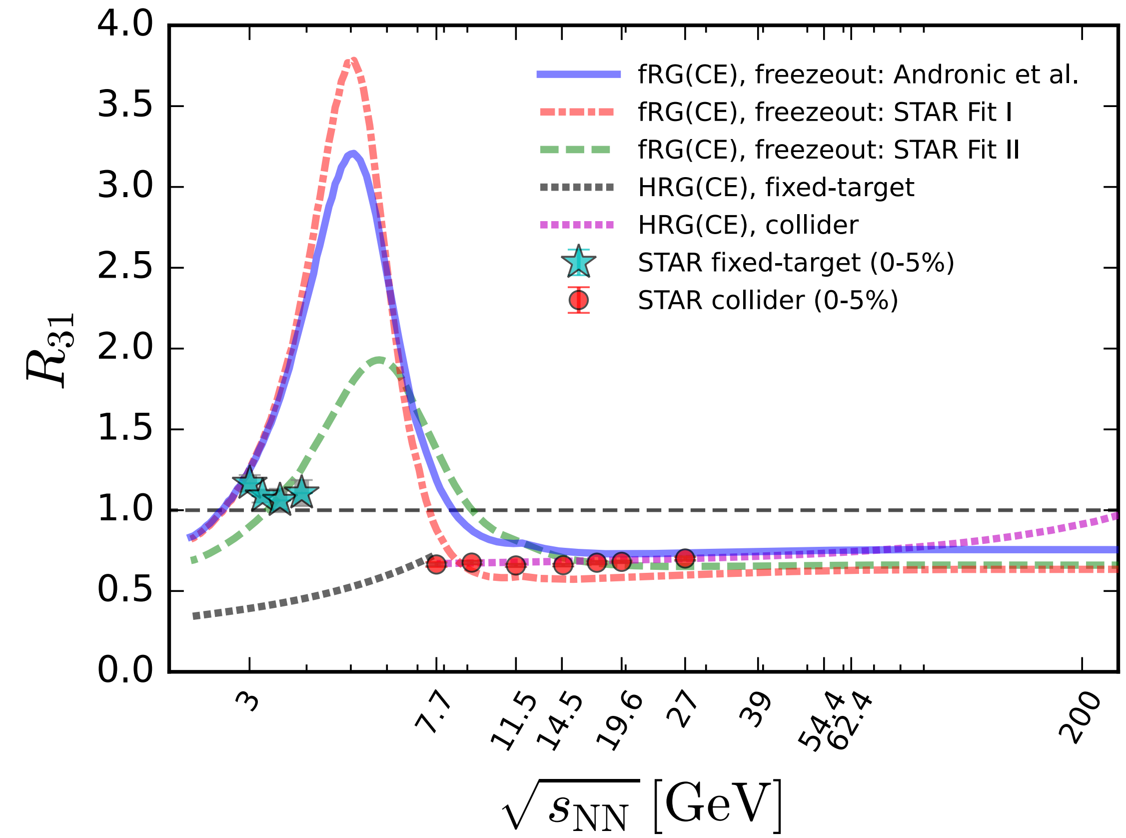

fRG: WF, Luo, Pawlowski, Rennecke, Yin, *PRD* 111 (2025) L031502, arXiv: 2308.15508; Zhao, Yin, WF, in preparation

- **Significant deviations from both the non-critical baseline results in UrQMD and HRG.**
- **fRG results are in accordance with data.**

κ_2/κ_1, κ_4/κ_1: factorial cumulants of proton

STAR data and UrQMD (baseline):

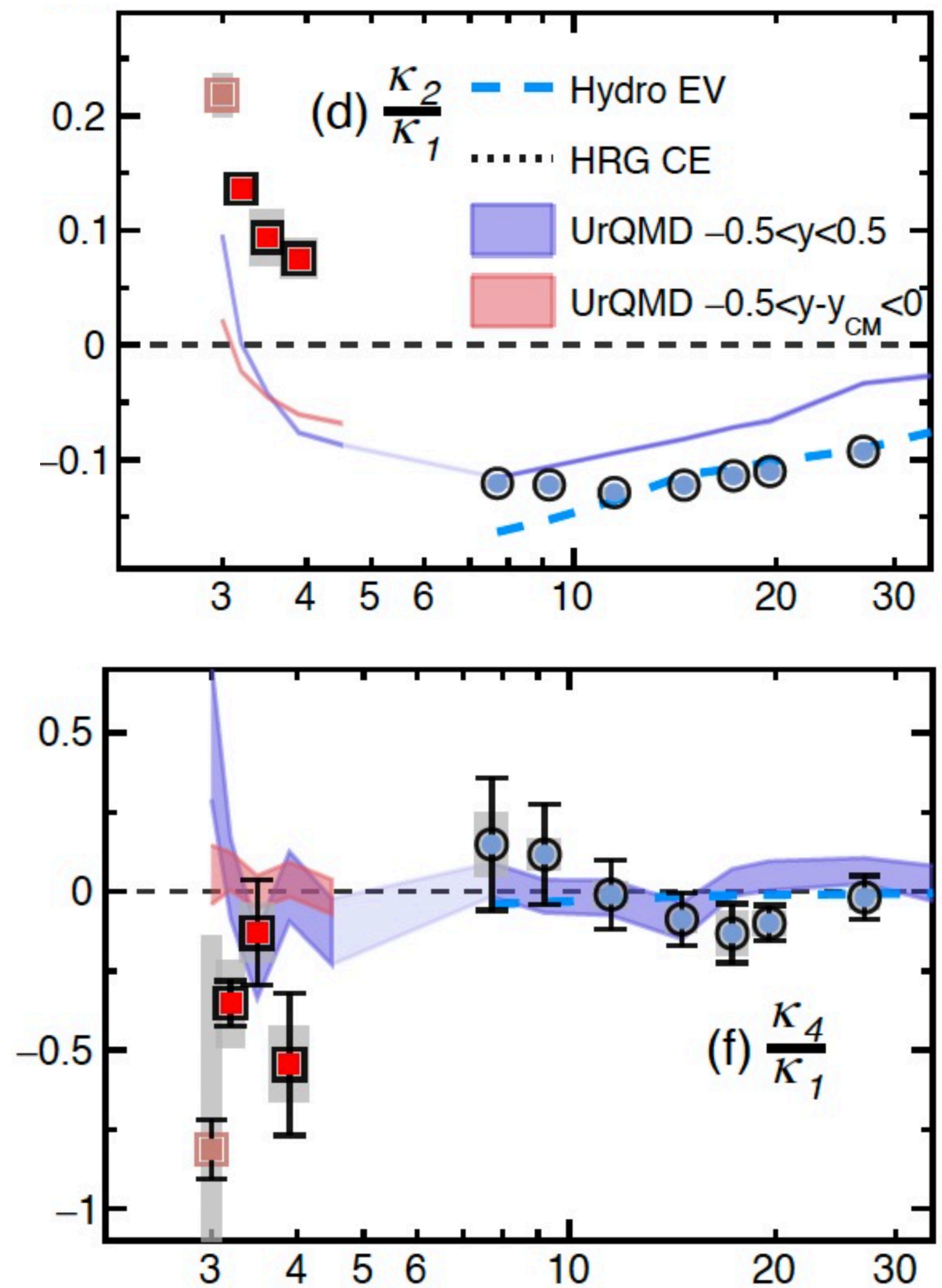

STAR: Z. Sweger, Quark Matter 2025

fRG (critical) and HRG (baseline):

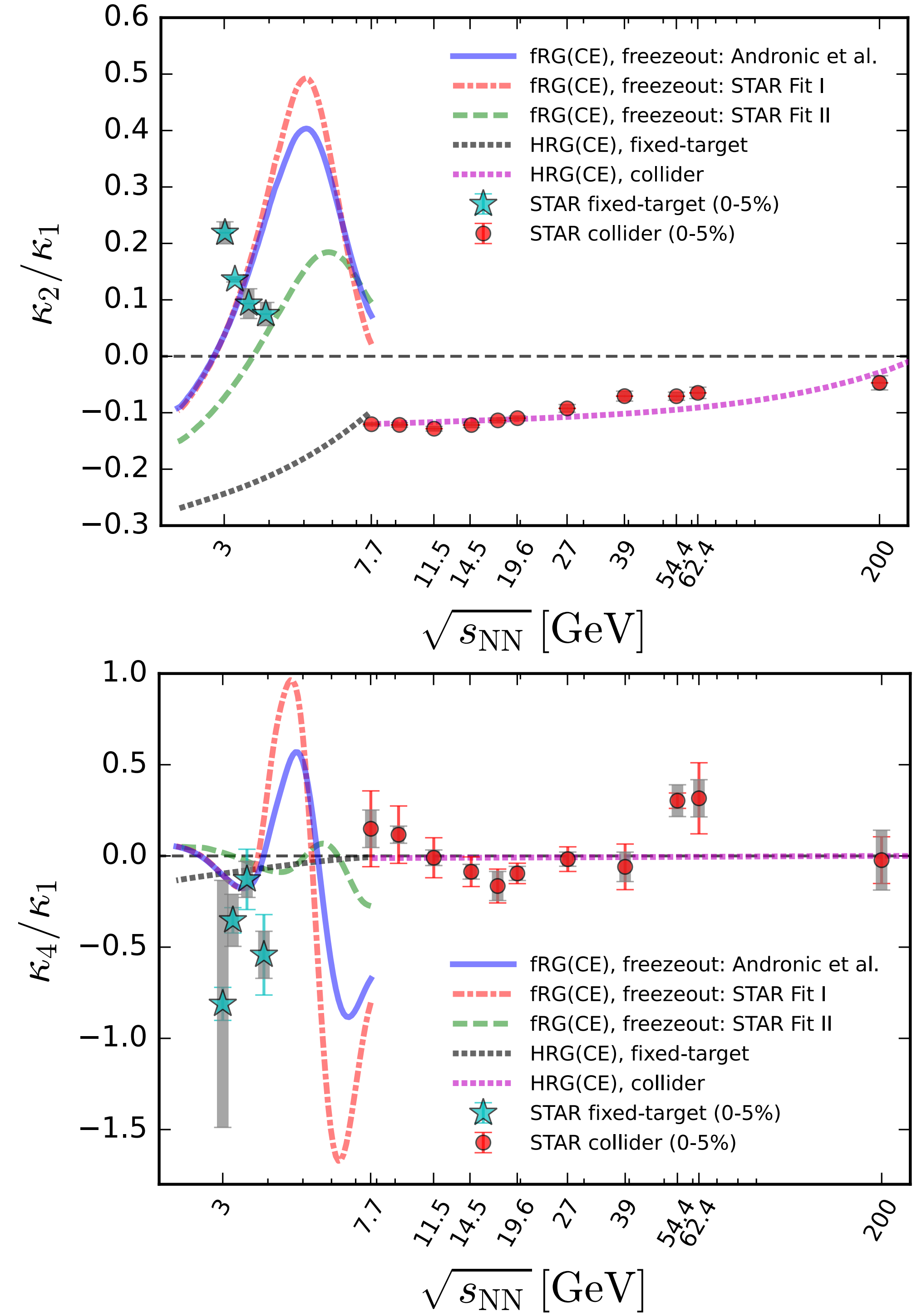

fRG and HRG: Zhao, Yin, WF, in preparation

- For κ_2/κ_1, the trend at fixed target is different for UrQMD and HRG.

κ_3/κ_1: factorial cumulants of proton

STAR data and UrQMD (baseline):

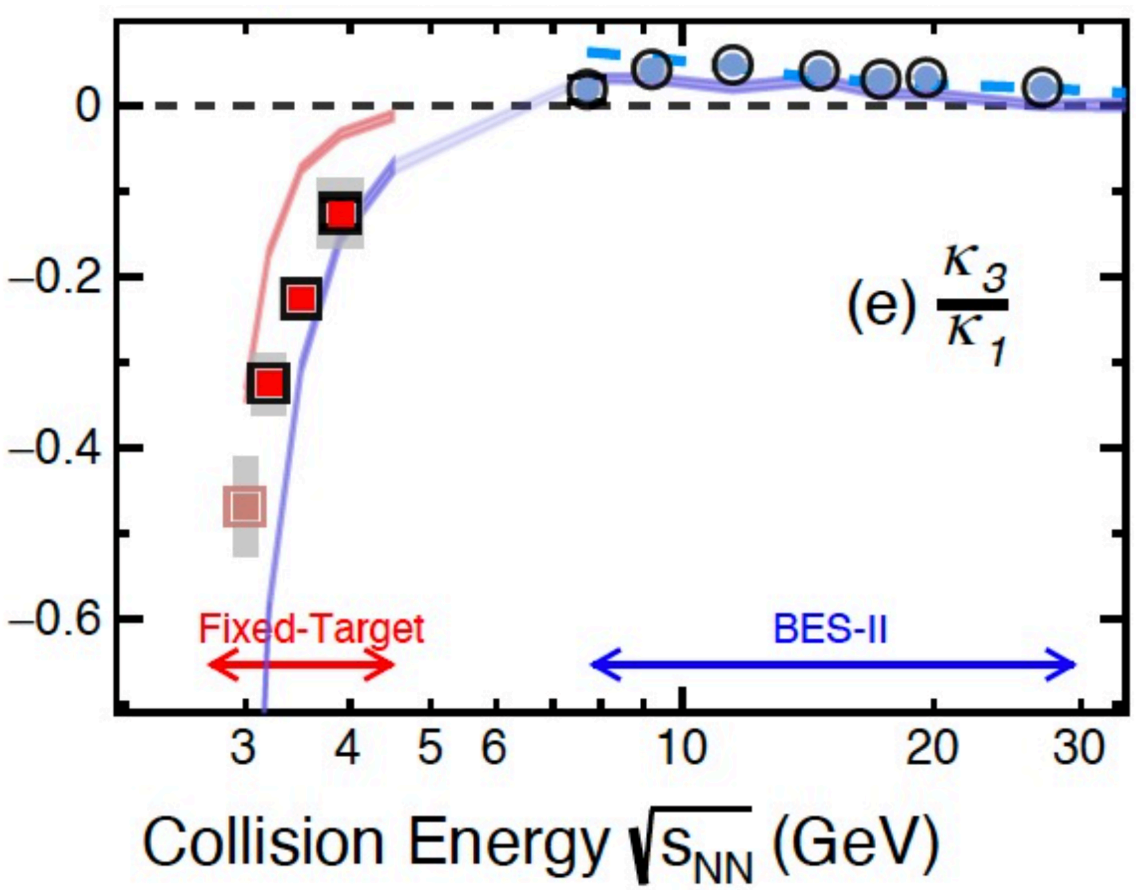

STAR: Z. Sweger, Quark Matter 2025

fRG (critical) and HRG (baseline):

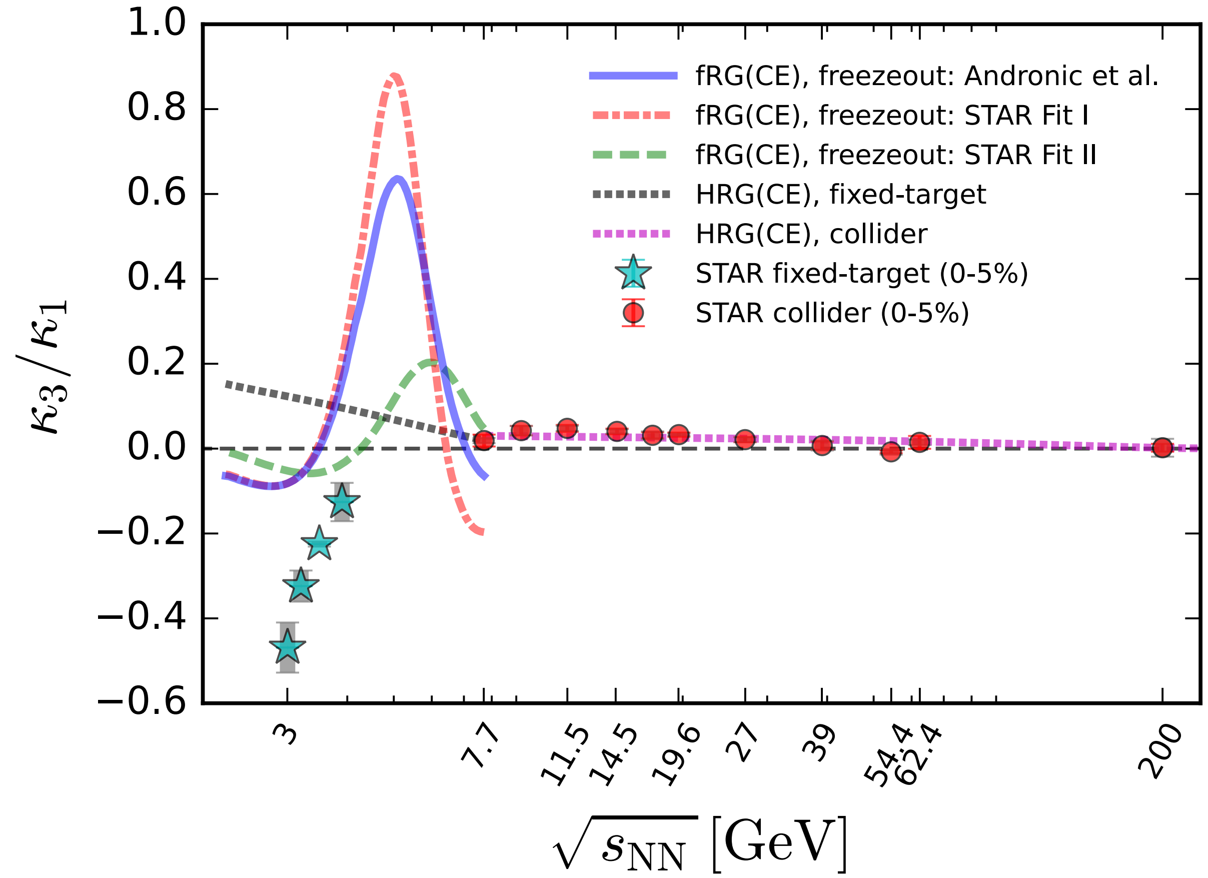

fRG and HRG: Zhao, Yin, WF, in preparation

- **The discrepancy between the UrQMD and HRG at the FXT energy might imply non-equilibrium effect becomes sizable at low collision energy?**

Spin fluctuations and correlations

Similarity between the spin and quark number:

$$\text{angular velocity} \quad \omega \Longleftrightarrow \mu \quad \text{chemical potential}$$
$$\text{conserved charge : spin} \quad S \Longleftrightarrow N \quad \text{quark number}$$

Then, one is able to obtain spin fluctuations and correlations arising from thermodynamics similarly as the quark number, e.g., the second-order quark-antiquark spin correlation

$$\langle P_q P_{\bar{q}} \rangle = \frac{4(\langle S_q S_{\bar{q}} \rangle - \langle S_q \rangle \langle S_{\bar{q}} \rangle)}{\sqrt{\langle N_q \rangle \langle N_{\bar{q}} \rangle}} = \frac{4C^S_{2,q\bar{q}}}{C^N_{1,q\bar{q}}}$$

With

$$C^S_{2,q\bar{q}} = VT\frac{\partial^2 p}{\partial \omega_q \omega_{\bar{q}}}, \qquad C^N_{1,q\bar{q}} = \sqrt{\langle N_q \rangle \langle N_{\bar{q}} \rangle} = V\left(\frac{\partial p}{\partial \mu_q}\frac{\partial p}{\partial \mu_{\bar{q}}}\right)^{1/2}$$

The kurtosis of spin fluctuations

$$\kappa\sigma^2 = \frac{C^S_4}{C^S_2}$$

With

$$C^S_n = VT^{n-1}\frac{\partial^n p}{\partial \omega^n}$$

Hao-Lei Chen, WF, Xu-Guang Huang, Guo-Liang Ma, *PRL* 135 (2025) 032302, arXiv:2410.20704.

Spin fluctuations and correlation

Second-order quark-antiquark spin correlation:

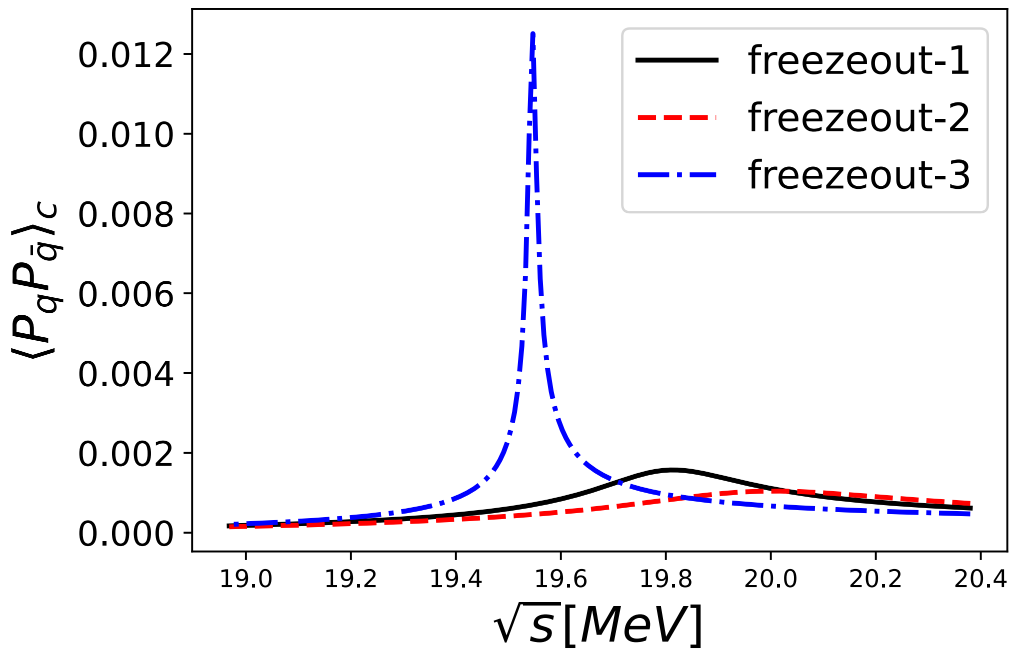

Kurtosis of spin fluctuation:

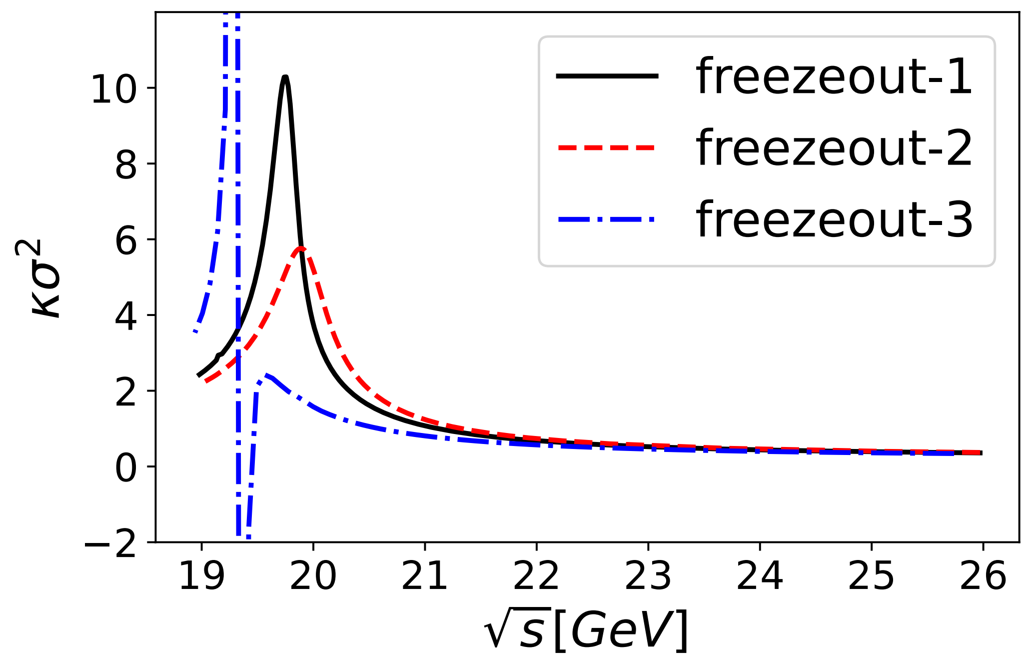

Hao-Lei Chen, WF, Xu-Guang Huang, Guo-Liang Ma, *PRL* 135 (2025) 032302, arXiv:2410.20704.

See the HENPIC talk by Hao-Lei Chen for more details, also refer to e.g., the references as follows

Z.-T. Liang and X.-N. Wang, *PRL* 94, 102301 (2005); *PLB* 629, 20 (2005).
X.-L. Sheng, L. Oliva, Z.-T. Liang, Q. Wang, and X.-N. Wang, *PRD* 101, 096005 (2020);X.-L. Sheng, L. Oliva, Z.-T. Liang, Q. Wang, and X.-N. Wang, *PRL* 131, 042304 (2023).
STAR, Nature 548, 62 (2017); Nature 614, 244 (2023).

Mean pt fluctuations

- The mean transverse momentum fluctuations of charged particles can be potentially used to probe the QCD thermodynamics and phase transitions.

Skewness of mean pt fluctuations:

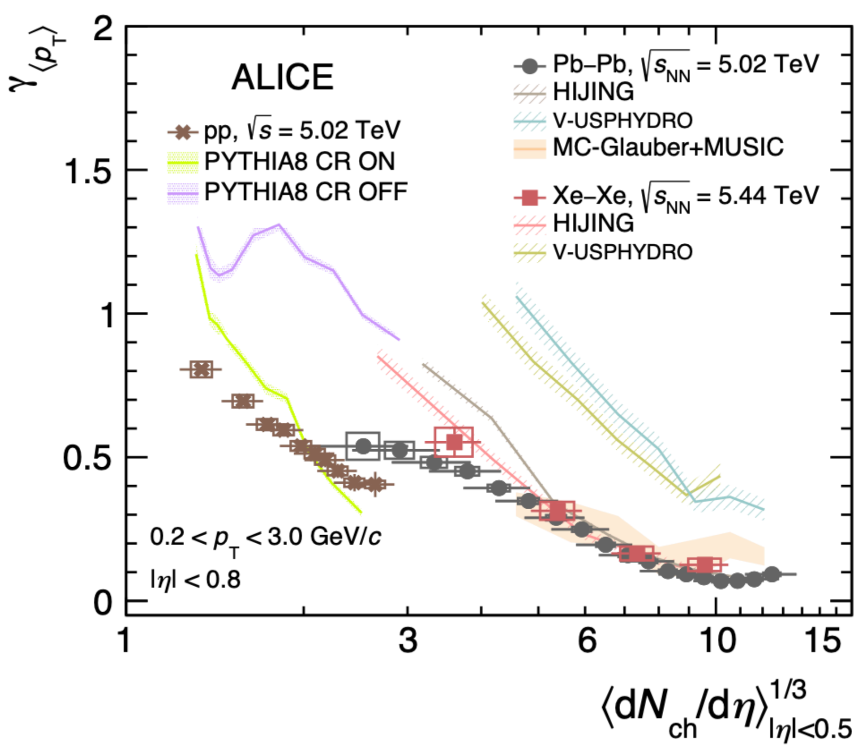

Kurtosis of mean pt fluctuations:

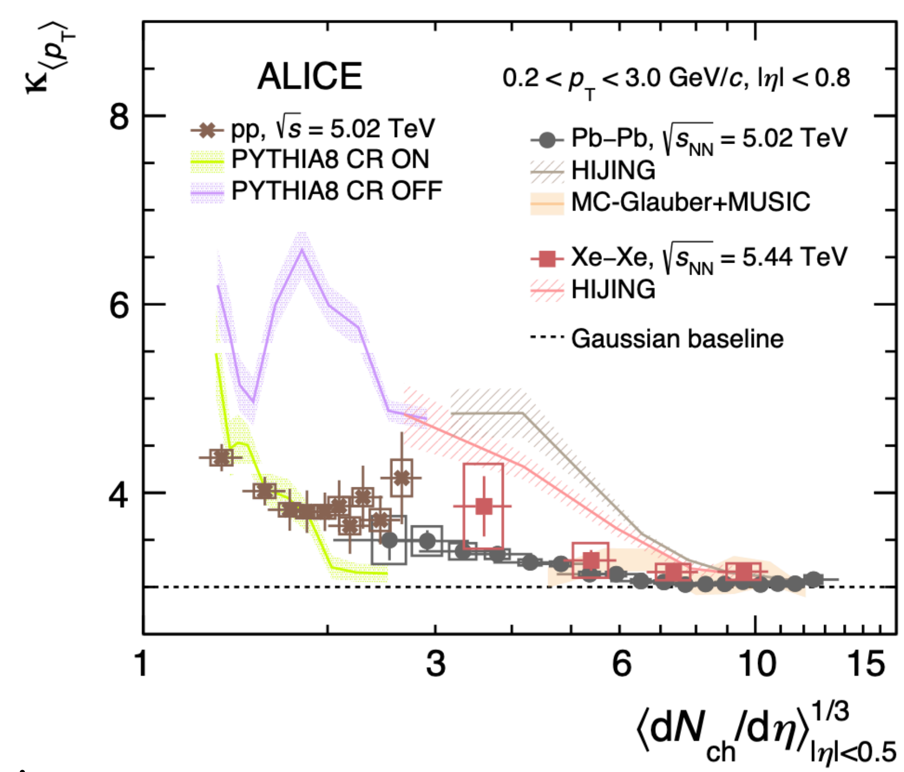

ALICE, *PLB* 850 (2024) 138541

We introduce a new thermodynamic state function

$$dW = TdS - pdV - N_B d\mu_B$$

With

$$W = \Omega + TS = U - \mu_B N_B$$

$N_{ch} \sim S$ is fixed, and V and μ_B are also fixed with some acceptance window. So, W is an appropriate state function to describe the experimental observables.

Derivation of temperature fluctuations

- Derivation of temperature fluctuations

From the state function W, the temperature and its fluctuations are be obtained

$$\frac{\partial w}{\partial s} = T$$

and

$$\langle (\Delta T)^n \rangle = T^{4n-4} \frac{\partial^n w}{\partial s^n}$$

It is convenient to adopt a dimensionless temperature fluctuation

$$c_n = \frac{\langle (\Delta T)^n \rangle}{T^n}$$

The first three nontrivial orders corresponding to the variance, skewness, and kurtosis of temperature fluctuations, are given by,

$$c_2 = T^2 \left(\frac{\partial^2 p}{\partial T^2} \right)^{-1}$$

$$c_3 = -T^5 \left(\frac{\partial^2 p}{\partial T^2} \right)^{-3} \frac{\partial^3 p}{\partial T^3}$$

$$c_4 = T^8 \left[3 \left(\frac{\partial^2 p}{\partial T^2} \right)^{-5} \left(\frac{\partial^3 p}{\partial T^3} \right)^{2} - \left(\frac{\partial^2 p}{\partial T^2} \right)^{-4} \frac{\partial^4 p}{\partial T^4} \right].$$

Jinhui Chen, WF, Shi Yin, Chunjian Zhang, arXiv:2504.06886

Temperature fluctuations

Variance of T fluctuations:

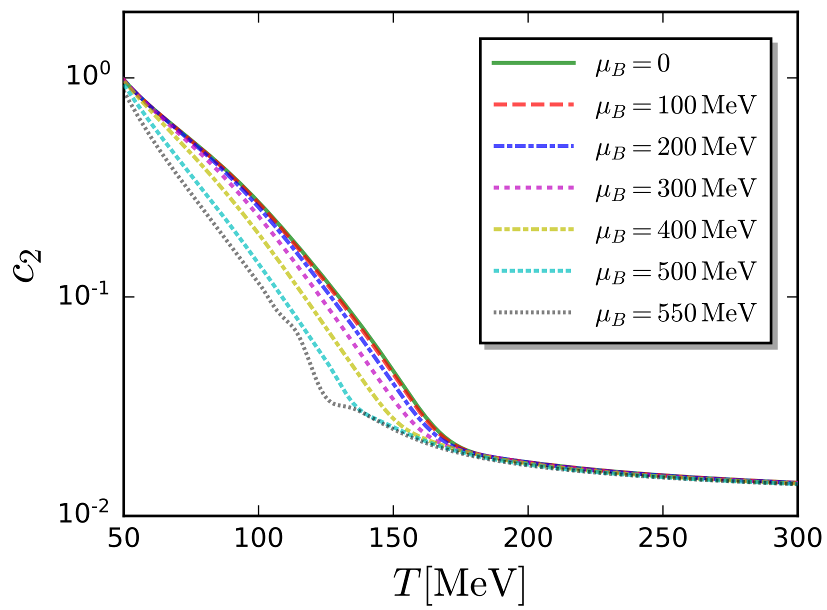

High-order T fluctuations:

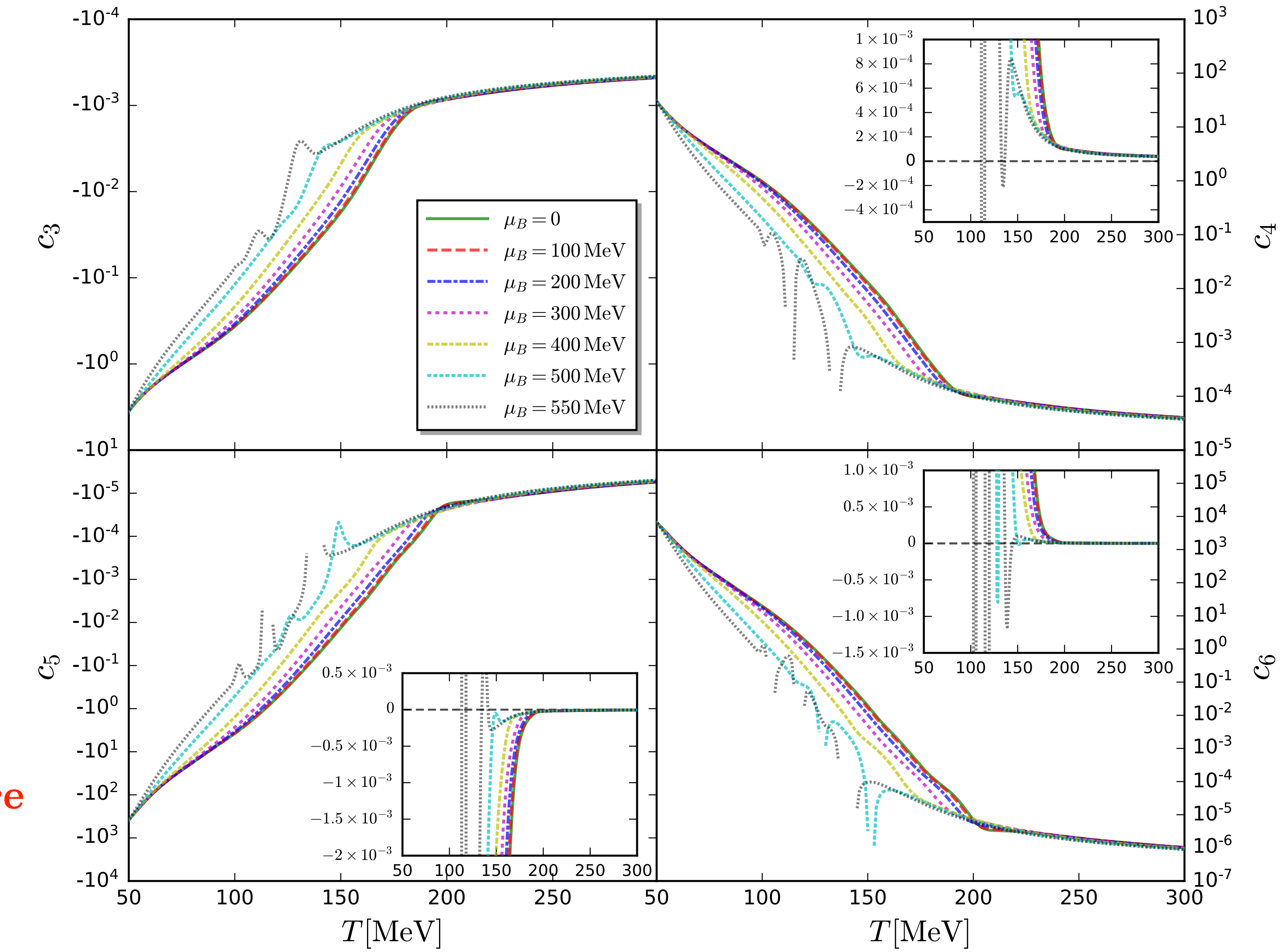

- **T fluctuations are suppressed remarkably as the system transitions from HRG to the QGP.**
- **Skewness of T fluctuations is negative, a smoking-gun signature of the temperature fluctuations.**
- **Due to the fact that the heat capacity of QGP is significantly larger than that of HRG**

Jinhui Chen, WF, Shi Yin, Chunjian Zhang, arXiv:2504.06886

Ratios of temperature fluctuations

Ratios of T fluctuations:

In order to avoid the influence of the proportionality constant a

$$\langle p_T \rangle = a\,T$$

It is more convenient to use the ratios of T fluctuations.

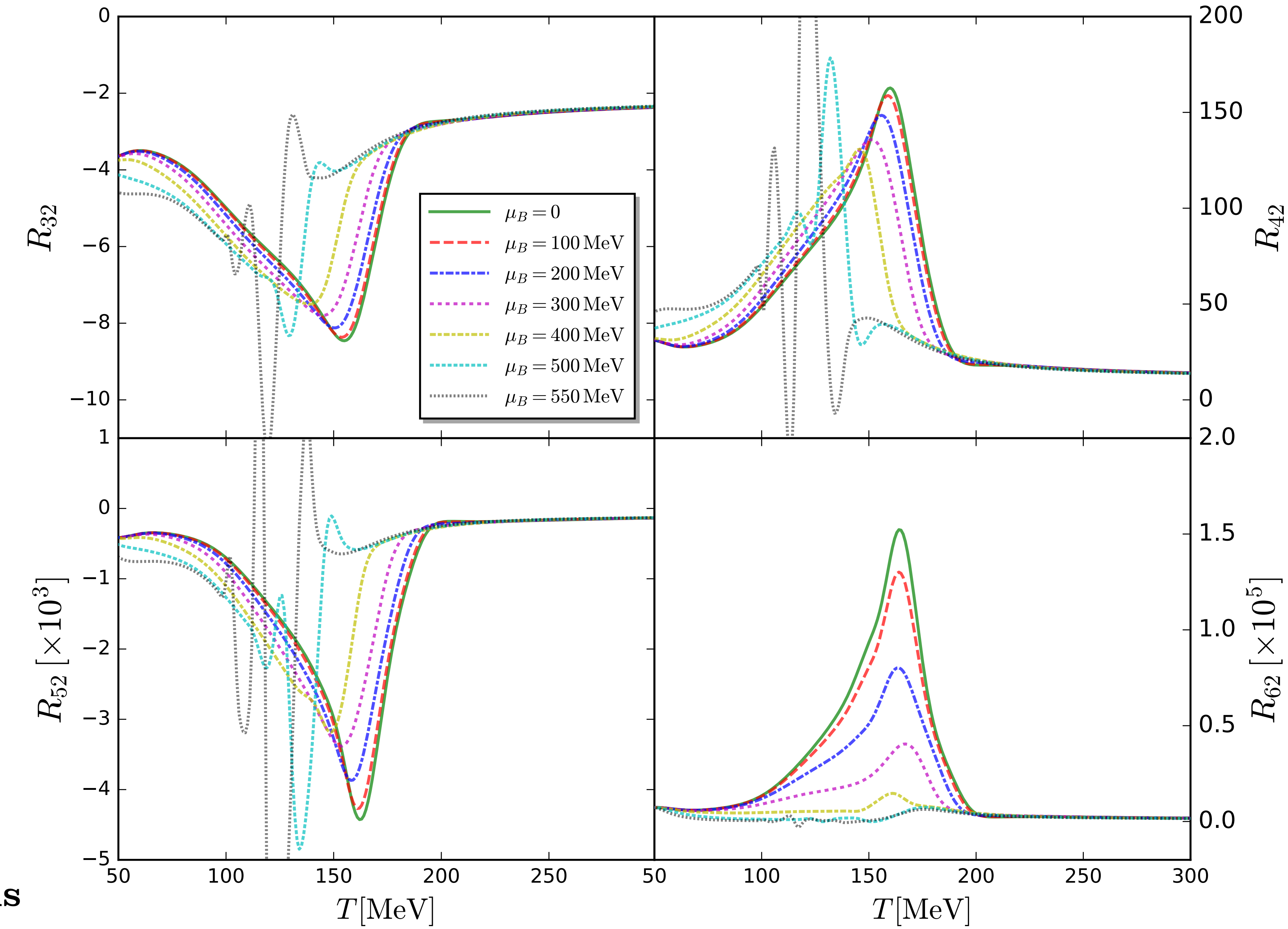

$$R_{32} = \frac{c_3}{c_2^2}, \quad R_{42} = \frac{c_4}{c_2^3}, \quad R_{52} = \frac{c_5}{c_2^4}, \quad R_{62} = \frac{c_6}{c_2^5}$$

Jinhui Chen, WF, Shi Yin, Chunjian Zhang, arXiv:2504.06886

- **Information of phase transitions are also encoded in these ratios.**
- **Can we use the temperature fluctuations to probe the QCD phase diagram?**

Schwinger-Keldysh path integral

- **Schrödinger equation:**

$$U(t,t_0) = e^{-iH(t-t_0)}$$

$$i\partial_t|\psi(t)\rangle = H|\psi(t)\rangle \quad \longrightarrow \quad |\psi(t)\rangle = U(t,t_0)|\psi(t_0)\rangle,$$

- **von Neumann equation:**

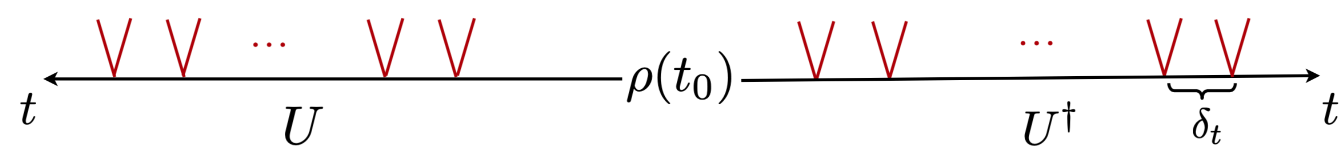

$$\partial_t\rho(t) = -i[H,\rho(t)] \quad \longrightarrow \quad \rho(t) = U(t,t_0)\rho(t_0)U^\dagger(t,t_0),$$

- **Keldysh partition function:**

$$Z = \mathrm{tr}\,\rho(t),$$

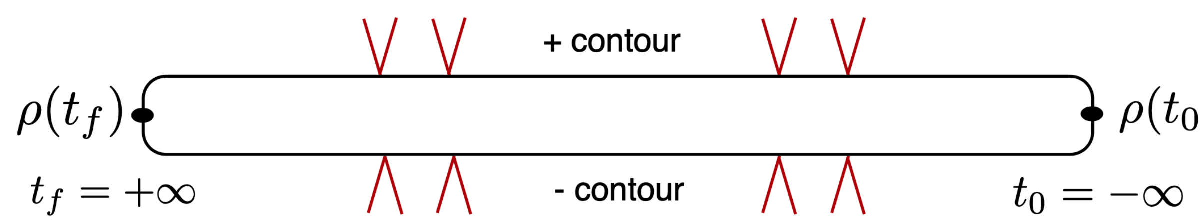

- **two-point closed time-path Green's function:**

$$G(x,y) \equiv -i\mathrm{tr}\{T_p(\phi(x)\phi^\dagger(y)\rho)\}$$
$$\equiv -i\langle T_p(\phi(x)\phi^\dagger(y))\rangle\,,$$

$$G(x,y) = \begin{pmatrix} G_{++} & G_{+-} \\ G_{-+} & G_{--} \end{pmatrix}$$
$$\equiv \begin{pmatrix} G_F & G_+ \\ G_- & G_{\tilde F} \end{pmatrix}\,,$$

$$G_F(x,y) \equiv -i\langle T(\phi(x)\phi^\dagger(y))\rangle\,,$$
$$G_+(x,y) \equiv -i\langle \phi^\dagger(y)\phi(x)\rangle\,,$$
$$G_-(x,y) \equiv -i\langle \phi(x)\phi^\dagger(y)\rangle\,,$$
$$G_{\tilde F}(x,y) \equiv -i\langle \tilde T(\phi(x)\phi^\dagger(y))\rangle\,,$$

Schwinger, J. Math. Phys. 2, 407 (1961);
Keldysh, Zh. Eksp. Teor. Fiz. 47, 1515 (1964);
Chou, Su, Hao, Yu, Phys. Rept. 118, 1 (1985).

FRG in Keldysh path integral

- **Implement the formalism of fRG in the two time branches:**

$$Z_k[J_c, J_q] = \int \left(\mathscr{D}\varphi_c \mathscr{D}\varphi_q\right) \exp\left\{ i\left(S[\varphi] + \Delta S_k[\varphi] + (J_q^i \varphi_{i,c} + J_c^i \varphi_{i,q}) \right) \right\},$$

with

$$\Delta S_k[\varphi] = \frac{1}{2}(\varphi_{i,c}, \varphi_{i,q}) \begin{pmatrix} 0 & R_k^{ij} \\ (R_k^{ij})^* & 0 \end{pmatrix} \begin{pmatrix} \varphi_{j,c} \\ \varphi_{j,q} \end{pmatrix}$$

$$= \frac{1}{2}\left(\varphi_{i,c} R_k^{ij} \varphi_{j,q} + \varphi_{i,q} (R_k^{ij})^* \varphi_{j,c} \right),$$

Keldysh rotation:

$$\begin{cases} \varphi_{i,+} = \frac{1}{\sqrt{2}}(\varphi_{i,c} + \varphi_{i,q}), \\ \varphi_{i,-} = \frac{1}{\sqrt{2}}(\varphi_{i,c} - \varphi_{i,q}), \end{cases}$$

- **Then we derive the flow equation in the closed time path:**

$$\partial_\tau \Gamma_k[\Phi] = \frac{i}{2} \mathrm{STr}\left[\left(\partial_\tau R_k^* \right) G_k \right],$$

$$R_k^{ab} \equiv \begin{pmatrix} 0 & R_k^{ij} \\ (R_k^{ij})^* & 0 \end{pmatrix},$$

$$iG(x,y) = \begin{pmatrix} iG^K(x,y) & iG^R(x,y) \\ iG^A(x,y) & 0 \end{pmatrix},$$

$$\boxed{\begin{aligned} iG^R(x,y) &= \theta(x^0 - y^0)\langle [\phi(x), \phi^*(y)] \rangle, \\ iG^A(x,y) &= \theta(y^0 - x^0)\langle [\phi^*(y), \phi(x)] \rangle, \\ iG^K(x,y) &= \langle \{ \phi(x), \phi^*(y) \} \rangle, \end{aligned}}$$

Tan, Chen, WF, *SciPost Phys*. 12 (2022) 026, arXiv: 2107.06482

A relaxation critical O(N) model

- **The effective action on the Schwinger-Keldysh contour reads**

Hohenberg and Halperin, *Rev. Mod. Phys*. 49 (1977) 435.

Model A

$$\Gamma[\phi_c,\phi_q] = \int d^4x \left(Z_a^{(t)}\,\phi_{a,q}\,\partial_t\,\phi_{a,c} - Z_a^{(i)}\,\phi_{a,q}\,\partial_i^2\,\phi_{a,c} + V'(\rho_c)\,\phi_{a,q}\,\phi_{a,c} - 2\,Z_a^{(t)}\,T\,\phi_{a,q}^2 - \sqrt{2}c\,\sigma_q \right)$$

$\Gamma = 1/Z_a^{(t)}$: relaxation rate

$V'(\rho_c)$: potential $\rho_c \equiv \phi_c^2/4$

$Z_a^{(i)}$: wave function

c: explicit breaking

Gaussian white noise with coefficient determined by fluctuation-dissipation theorem

- **Retarded propagator**

$$G_{ab}^R = \left(\frac{\delta^2\Gamma[\phi_c,\phi_q]}{\delta\phi_{a,q}\,\delta\phi_{b,c}} \right)^{-1}$$

Retarded propagator of Goldstone

$$G_{\varphi\varphi}^R(\omega,q) = \frac{1}{-\mathrm{i}Z_\varphi^{(t)}\omega + Z_\varphi^{(i)}\left(q^2 + m_\varphi^2\right)}$$

pseudo-Goldstone:

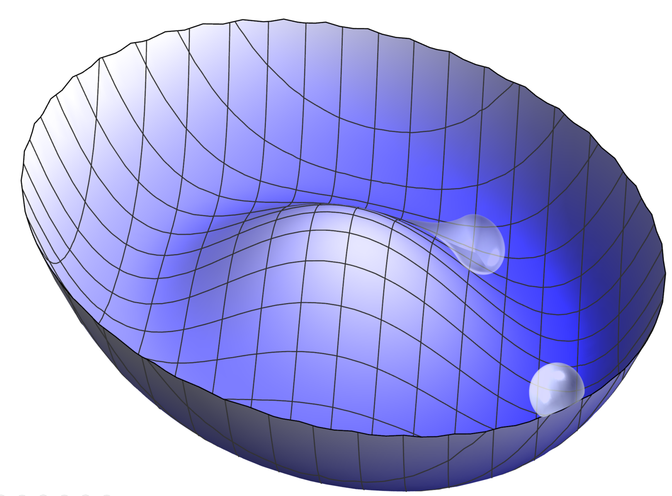

Mass of pseudo-Goldstone

$$m_\varphi^2 = \frac{V'(\rho_0)}{Z_\varphi^{(i)}} = \frac{c}{\sigma_0 Z_\varphi^{(i)}}$$

Gell-Mann--Oakes--Renner (GMOR) relation

Universal damping or not?

From the pole of the retarded propagator of Goldstone

$$G^R_{\varphi\varphi}(\omega, q) = \frac{1}{-\mathrm{i}Z^{(t)}_\varphi \omega + Z^{(i)}_\varphi \left(q^2 + m^2_\varphi\right)}$$

One obtains the dispersion relation of a damped mode

$$\omega(q) = -\,\mathrm{i}\,\frac{Z^{(i)}_\varphi}{Z^{(t)}_\varphi}\left(m^2_\varphi + q^2\right)$$

The relaxation rate at zero momentum reads

$$\Omega_\varphi \equiv -\,\mathrm{Im}\,\omega(q=0) = \frac{Z^{(i)}_\varphi}{Z^{(t)}_\varphi}\,m^2_\varphi$$

- **If** $T \ll T_c$

$$\frac{\Omega_\varphi}{m^2_\varphi} \simeq D_\varphi(T) + \mathcal{O}\left(\frac{m^2_\varphi}{T^2}\right) \quad \textbf{with} \quad D_\varphi(T) \equiv \frac{Z^{(i)}_\varphi(T, c=0)}{Z^{(t)}_\varphi(T, c=0)}$$

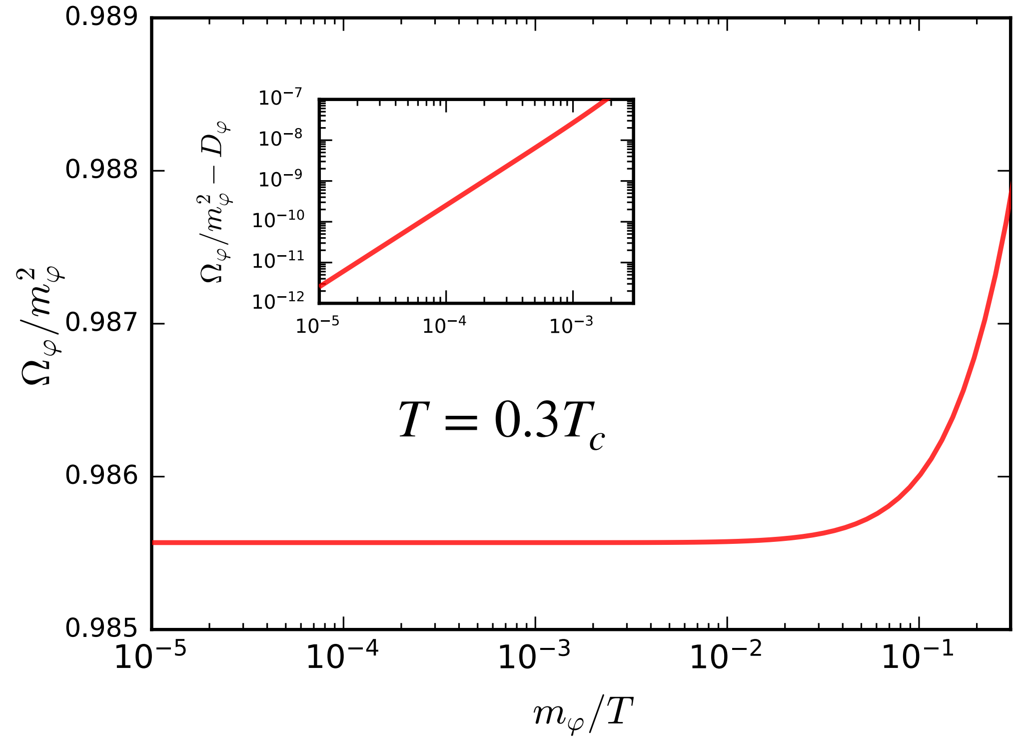

Tan, Chen, WF, Li, *Nature Commun.* 16 (2025) 2916, arXiv: 2403.03503

This seemingly appears as a **universal** relation that was also observed in Holographics, Hydrodynamics, and EFT

Holographics:
Amoretti, Areán, Goutéraux, Musso, *PRL* 123 (2019) 211602;
Amoretti, Areán, Goutéraux, Musso, *JHEP* 10 (2019) 068;
Ammon *et al*., *JHEP* 03 (2022) 015;
Cao, Baggioli, Liu, Li, *JHEP* 12 (2022) 113

Hydrodynamics:
Delacrétaz, Goutéraux, Ziogas, *PRL* 128 (2022) 141601

EFT:
Baggioli, *Phys. Rev. Res.* 2 (2020) 022022;
Baggioli, Landry, *SciPost Phys*. 9 (2020) 062

Emergence of a novel universal damping in the critical region

In the critical region, the two wave function renormalizations read

$$Z_\varphi^{(i)} = t^{-\nu\eta} f^{(i)}(z)\,, \qquad Z_\varphi^{(t)} = t^{-\nu\eta_t} f^{(t)}(z)$$

Here $f^{(i)}(z), f^{(t)}(z)$: scaling functions; $z \equiv tc^{-1/(\beta\delta)}$: scaling variable; $t \equiv (T_c - T)/T_c$: reduced temperature.The static and dynamic anomalous dimensions are

$$\eta = -\frac{\partial_\tau Z_\varphi^{(i)}}{Z_\varphi^{(i)}}\,, \qquad \eta_t = -\frac{\partial_\tau Z_\varphi^{(t)}}{Z_\varphi^{(t)}}$$

RG time $\tau = \ln(k/\Lambda)$

- In the case of $c \to 0$

$$\frac{Z_\varphi^{(i)}}{Z_\varphi^{(t)}} \propto t^{\nu(\eta_t - \eta)}$$

- In the other case of $t \to 0$

$$\frac{Z_\varphi^{(i)}}{Z_\varphi^{(t)}} \propto c^{\frac{\nu}{\beta\delta}(\eta_t - \eta)} \propto m_\varphi^{(\eta_t - \eta)} \quad \text{with} \quad m_\varphi^2 \propto c^{\frac{2\nu}{\beta\delta}}$$

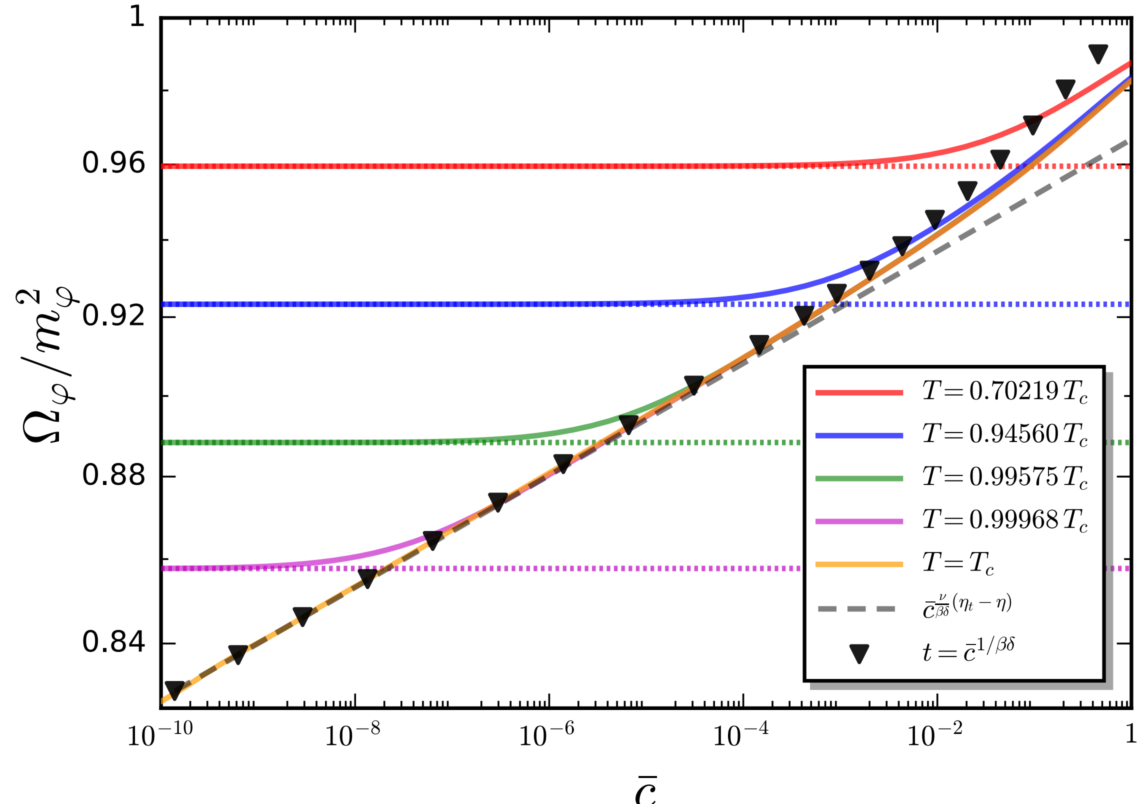

Tan, Chen, WF, Li, *Nature Commun.* 16 (2025) 2916, arXiv: 2403.03503

From the fixed-point equation we determine in the O(4) symmetry

$$\eta \approx 0.0374, \quad \eta_t \approx 0.0546$$

Thus

$$\Delta_\eta \equiv \eta_t - \eta \approx 0.0172$$

Estimate of size of the dynamic critical region:

$$m_{\pi 0} \lesssim 0.1 \sim 1\ \text{MeV}$$

Large N limit

In the large N limit, the static and dynamic anomalous dimensions can be solved analytically

$$\eta = \frac{5}{N-1}\frac{(1+\eta)(1-2\eta)^2}{(5-\eta)(2-\eta)^2}$$

and

$$\eta_t = \frac{1}{9(N-1)}\frac{(1-2\eta)^2(13+15\eta-2\eta^3)}{(2-\eta)^2}$$

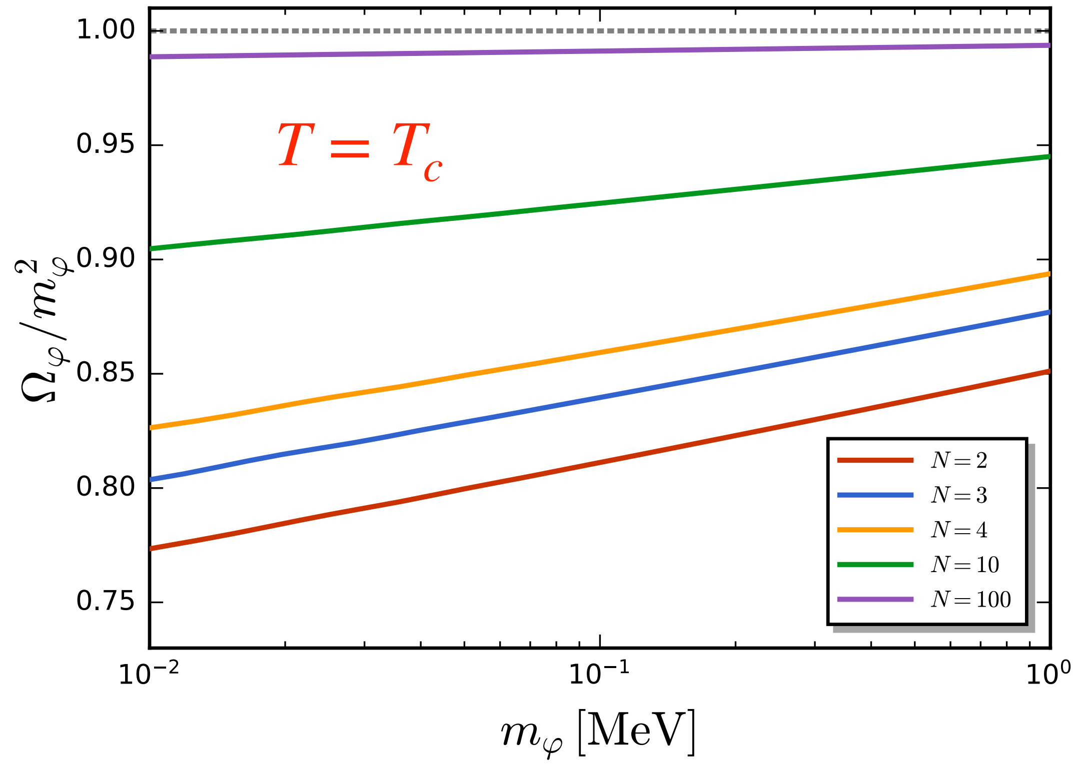

Tan, Chen, WF, Li, *Nature Commun.* 16 (2025) 2916, arXiv: 2403.03503

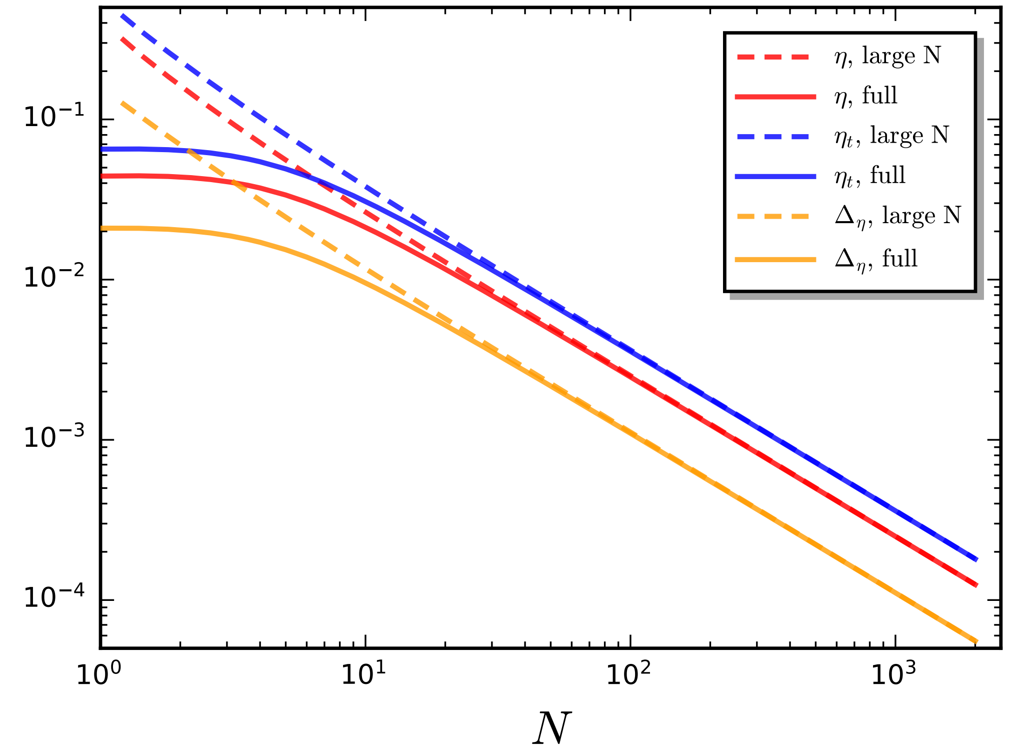

- In the limit $N \to \infty$, the novel universal damping disappears.
- One should not expect that the anomalous scaling regime can be observed in classical holographic models.

Relaxation dynamics of the critical mode

- Langevin dynamics of the critical mode:

$$Z_\phi^{(t)}\partial_t\sigma - Z_\phi^{(i)}\partial_i^2\sigma + U'(\sigma) = \xi$$

with the correlation of the Gaussian white noise

$$\langle \xi(t,\boldsymbol{x})\xi(t',\boldsymbol{x}')\rangle = 2\, Z_\phi^{(t)}\, T\,\delta(t-t')\delta(\boldsymbol{x}-\boldsymbol{x}')$$

- Inputs from first-principles functional QCD: WF, Pawlowski, Rennecke, *PRD* 101 (2020) 054032

Effective potential:

$$U'(\sigma) = \left.\frac{\delta\Gamma[\Phi]}{\delta\sigma}\right|_{\substack{\sigma(x)=\sigma \\ \tilde{\Phi}=\tilde{\Phi}_{\mathrm{EoM}}}}$$

Spatial wave function:

$$Z_\phi^{(i)} = \left.\frac{\partial\Gamma^{(2)}_{\sigma\sigma}(p_0,\boldsymbol{p})}{\partial\boldsymbol{p}^2}\right|_{\substack{p_0=0 \\ \boldsymbol{p}=0}}$$

Temporal wave function:

$$Z_\phi^{(t)} = \lim_{|\boldsymbol{p}|\to 0}\lim_{\omega\to 0}\frac{\partial}{\partial\omega}\mathrm{Im}\,\Gamma^{(2)}_{\sigma\sigma,\mathrm{R}}(\omega,\boldsymbol{p})$$

with

$$\Gamma^{(2)}_{\sigma\sigma,\mathrm{R}}(\omega,\boldsymbol{p}) = \lim_{\epsilon\to 0^+}\Gamma^{(2)}_{\sigma\sigma}\big(p_0=-\mathrm{i}(\omega+\mathrm{i}\epsilon),\boldsymbol{p}\big)$$

Relaxation time in QCD phase diagram

Relaxation time:

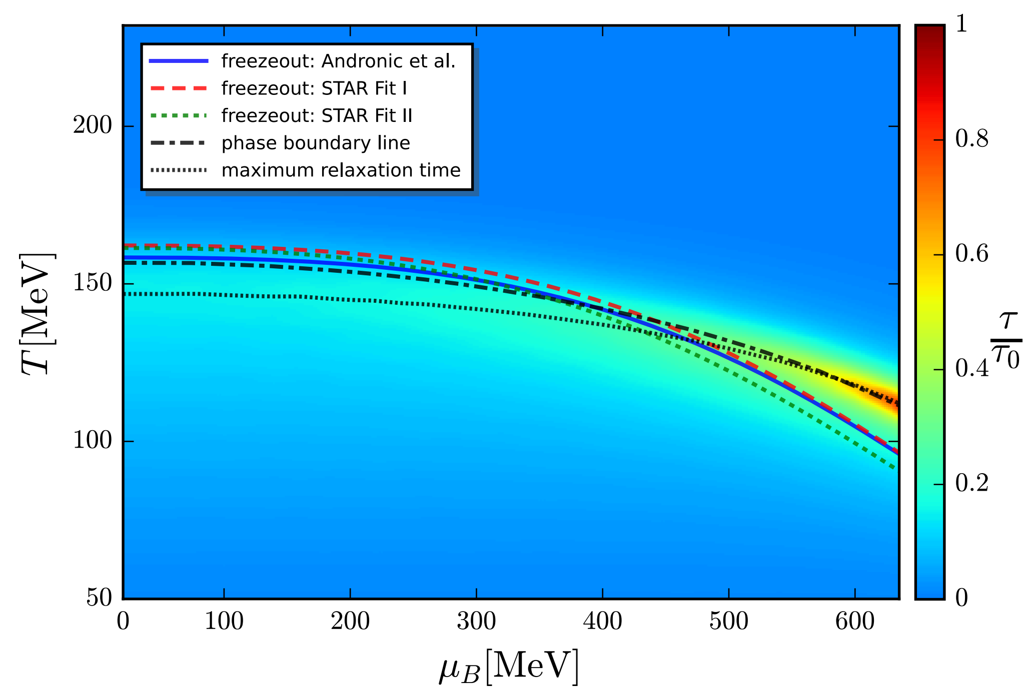

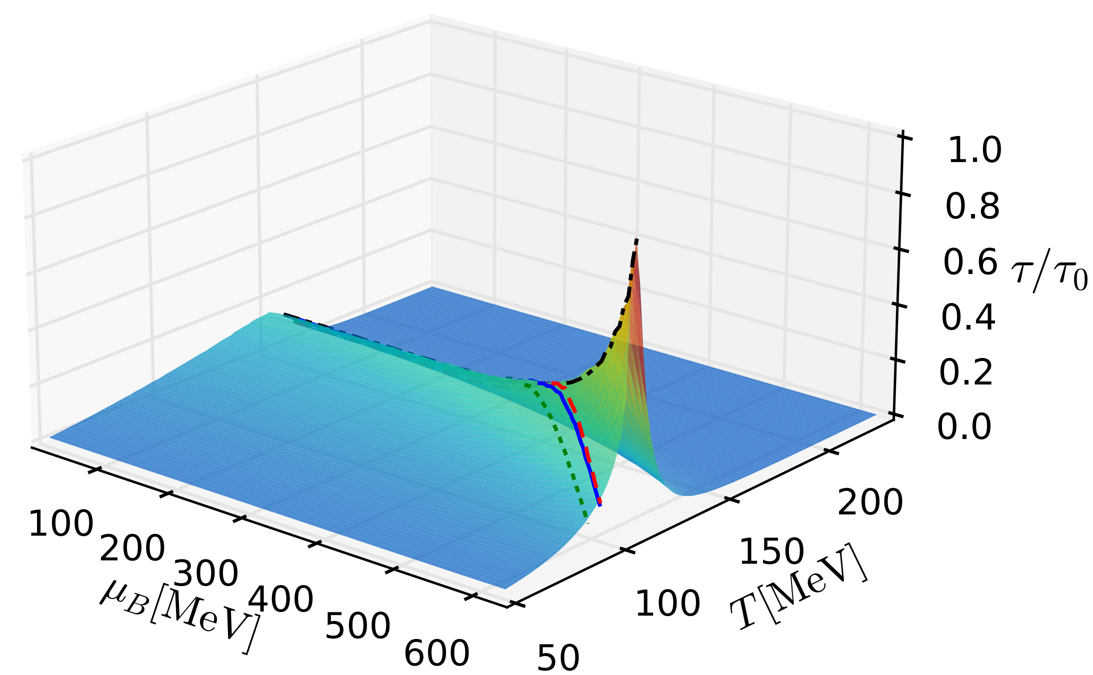

Tan, Yin, Chen, Huang, WF, in preparation

Relaxation time at the freezeout :

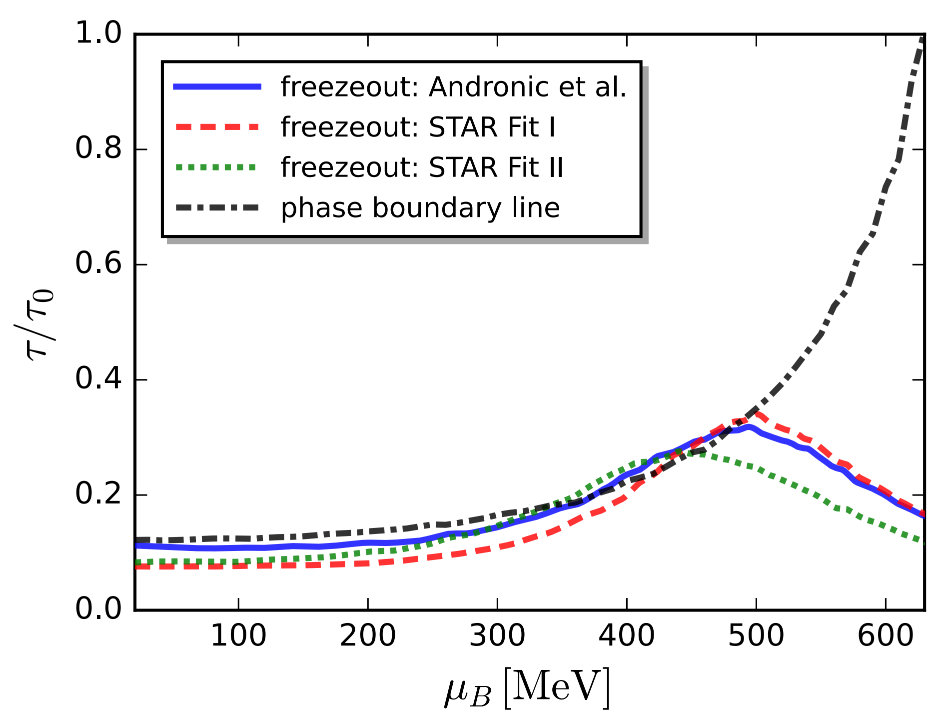

See also:
M. Bluhm *et al.*, *NPA* 982 (2019) 871

- Relaxation time drops quickly once the system is away from the critical regime.

Summary and outlook

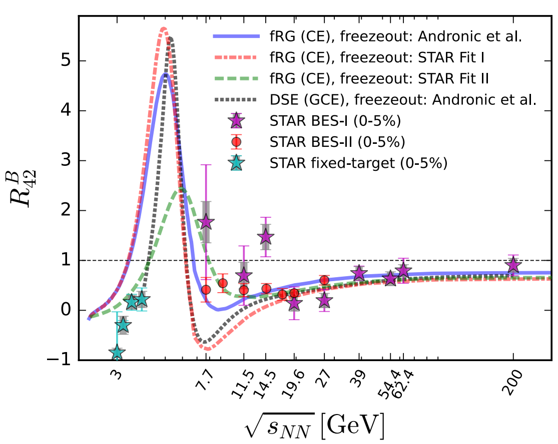

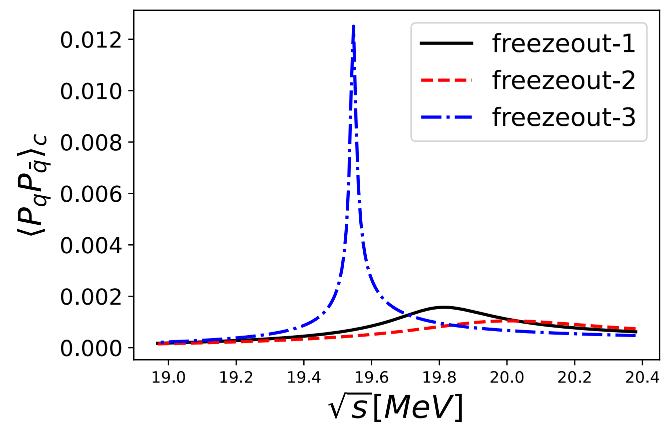

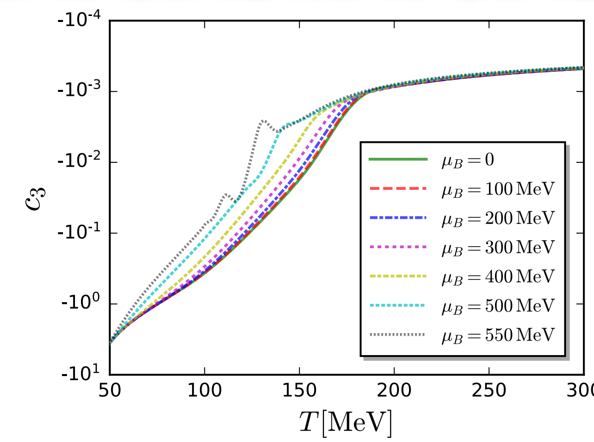

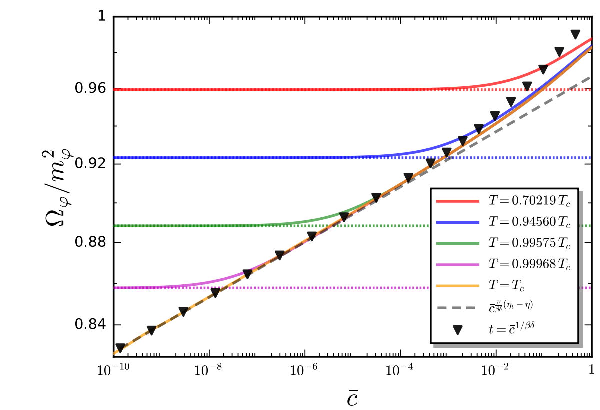

★ A prominent peak structure is predicted in baryon number fluctuations in the collision energy range of 3 GeV $\lesssim \sqrt{s_{\mathrm{NN}}} \lesssim$ 7.7 GeV, which need to be confirmed in experiments in the near future.

★ Spin fluctuations and correlations are promising probes to QCD thermodynamics.

★ A negative skewness of mean p_t fluctuations is potentially a smoking-gun signature of the temperature fluctuations.

★ A novel universal damping in the critical region is found.

Summary and outlook

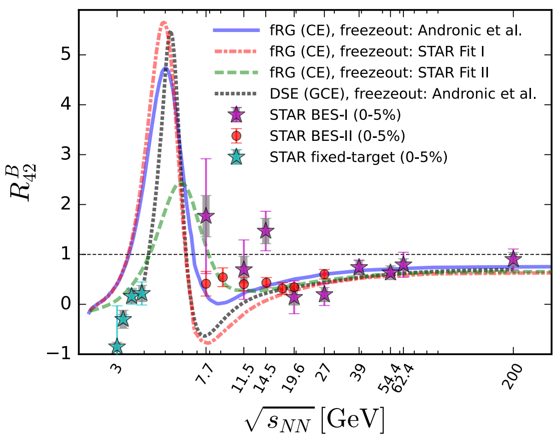

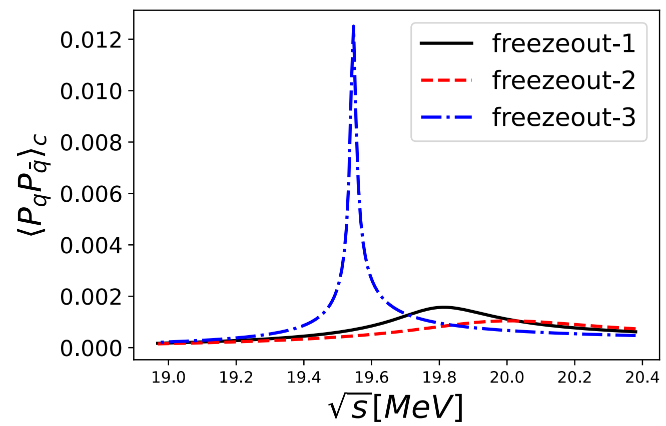

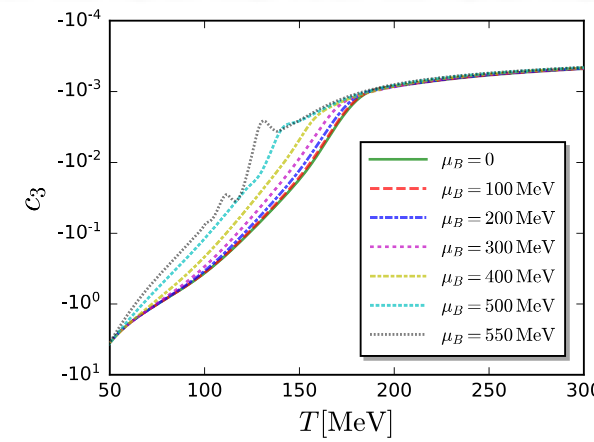

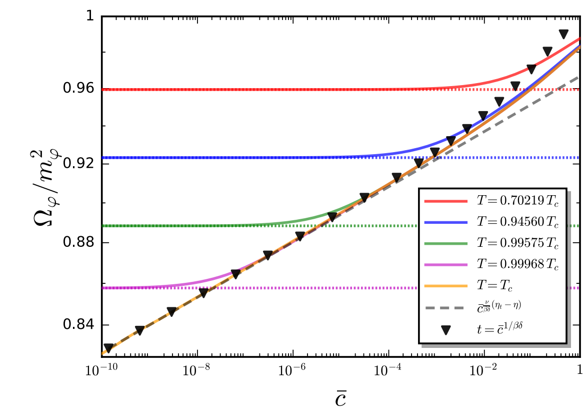

★ A prominent peak structure is predicted in baryon number fluctuations in the collision energy range of 3 GeV $\lesssim \sqrt{s_{\mathrm{NN}}} \lesssim$ 7.7 GeV, which need to be confirmed in experiments in the near future.

★ Spin fluctuations and correlations are promising probes to QCD thermodynamics.

★ A negative skewness of mean p_t fluctuations is potentially a smoking-gun signature of the temperature fluctuations.

★ A novel universal damping in the critical region is found.

Thank you very much for your attentions!

Backup

QCD-assisted LEFT

QCD flow equation:

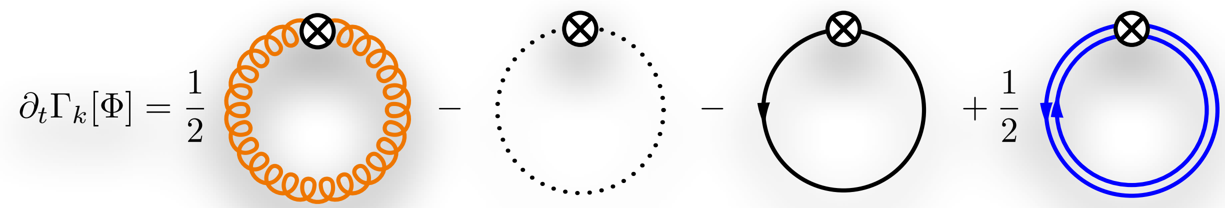

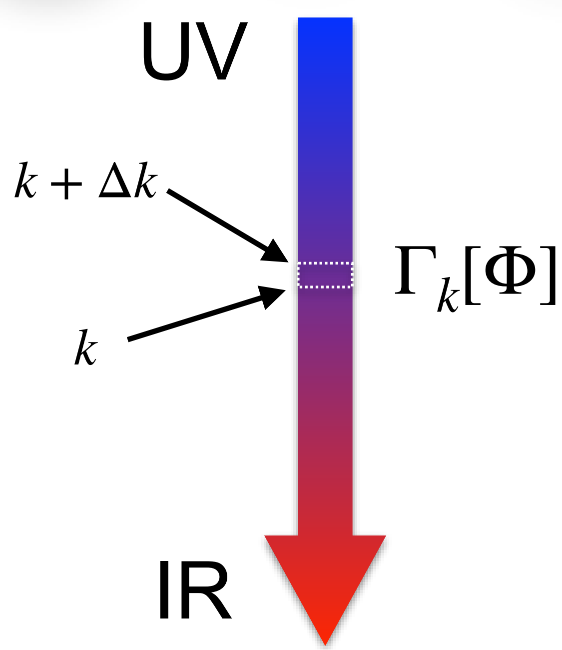

LEFT flow equation:

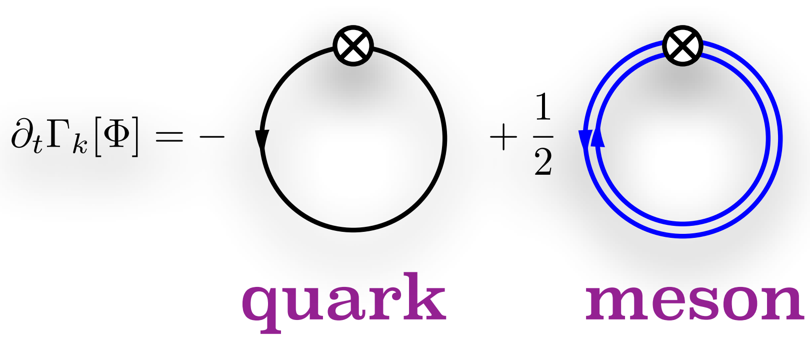

- **Yukawa couplings obtained in QCD inputted in QCD-assisted LEFT**

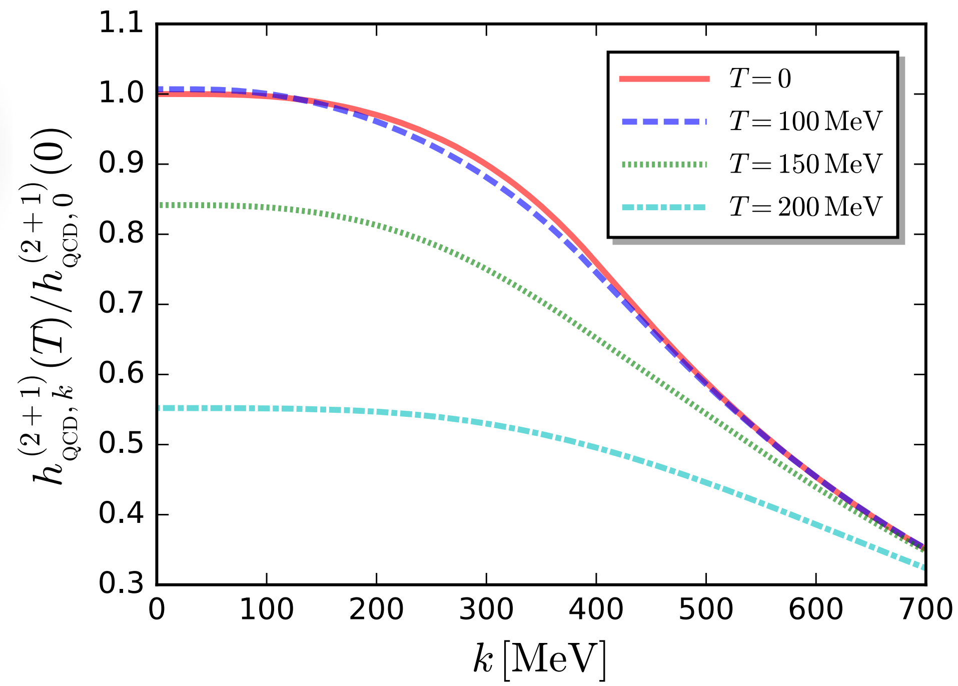

WF, Pawlowski, Rennecke, *PRD* 101 (2020) 054032

- **Chiral condensates in QCD and QCD-assisted LEFT in agreement**

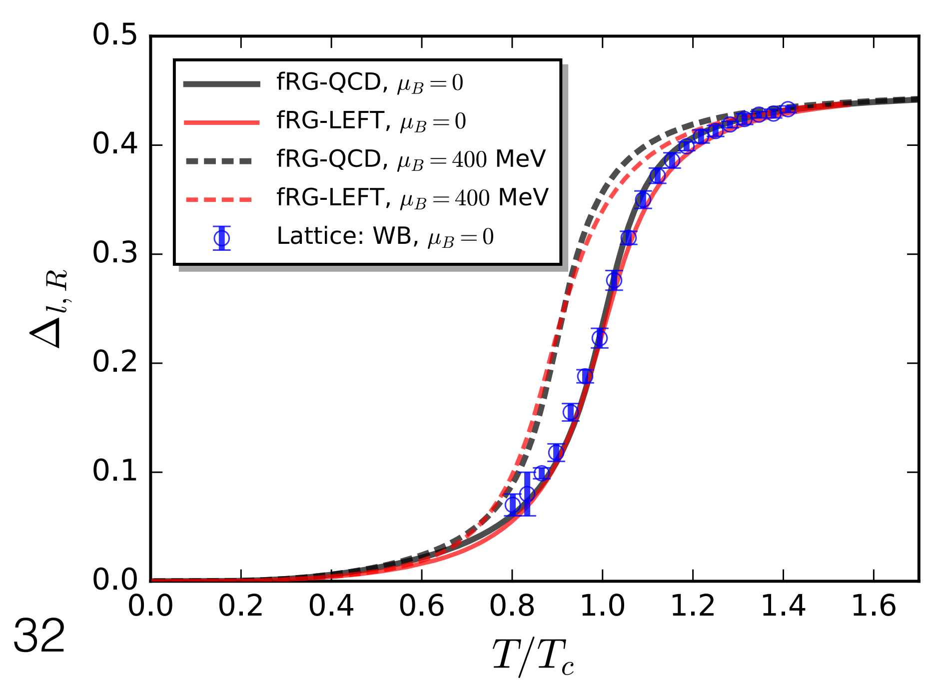

WF, Luo, Pawlowski, Rennecke, Yin, arXiv: 2308.15508

Grand canonical fluctuations at the freeze-out

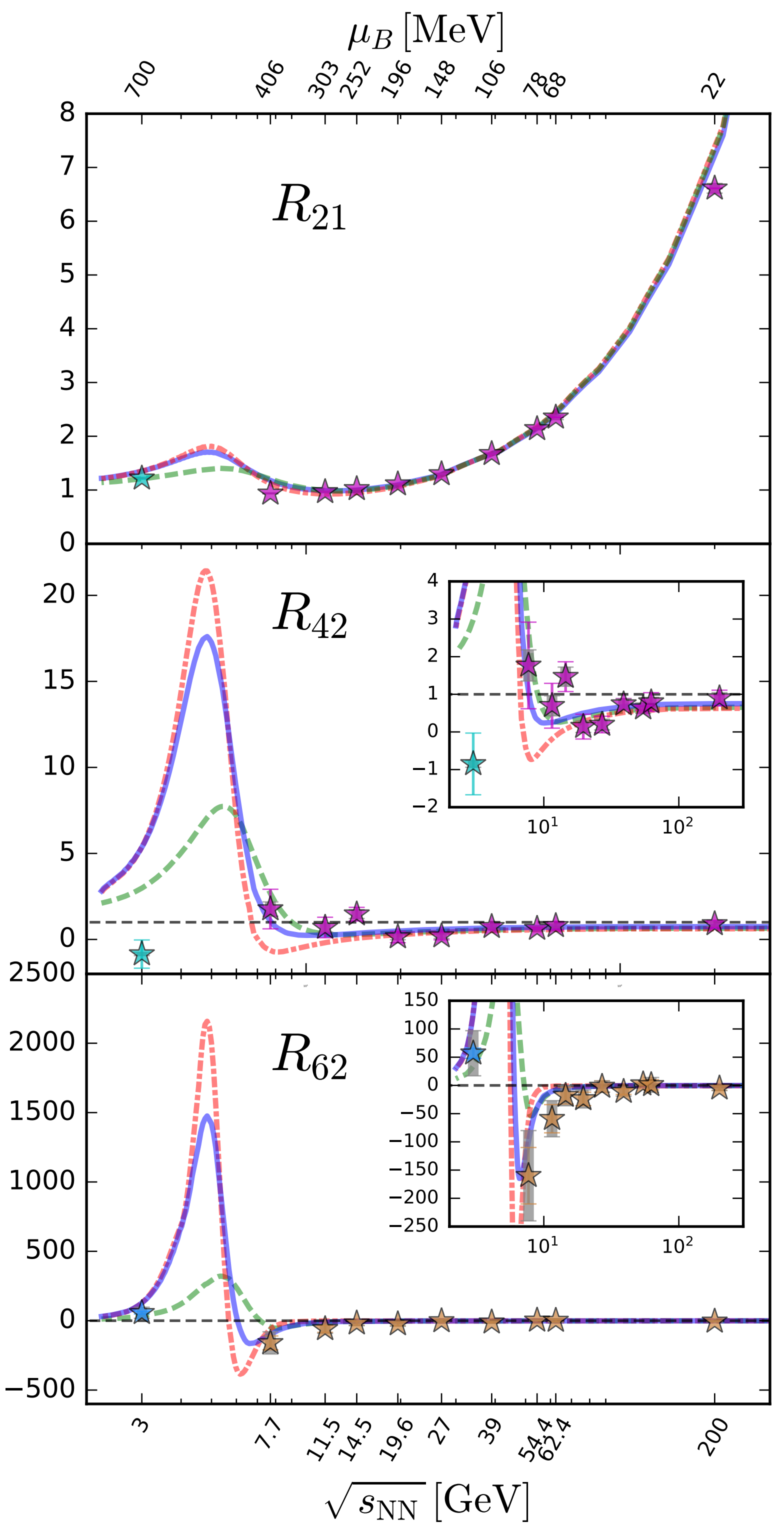

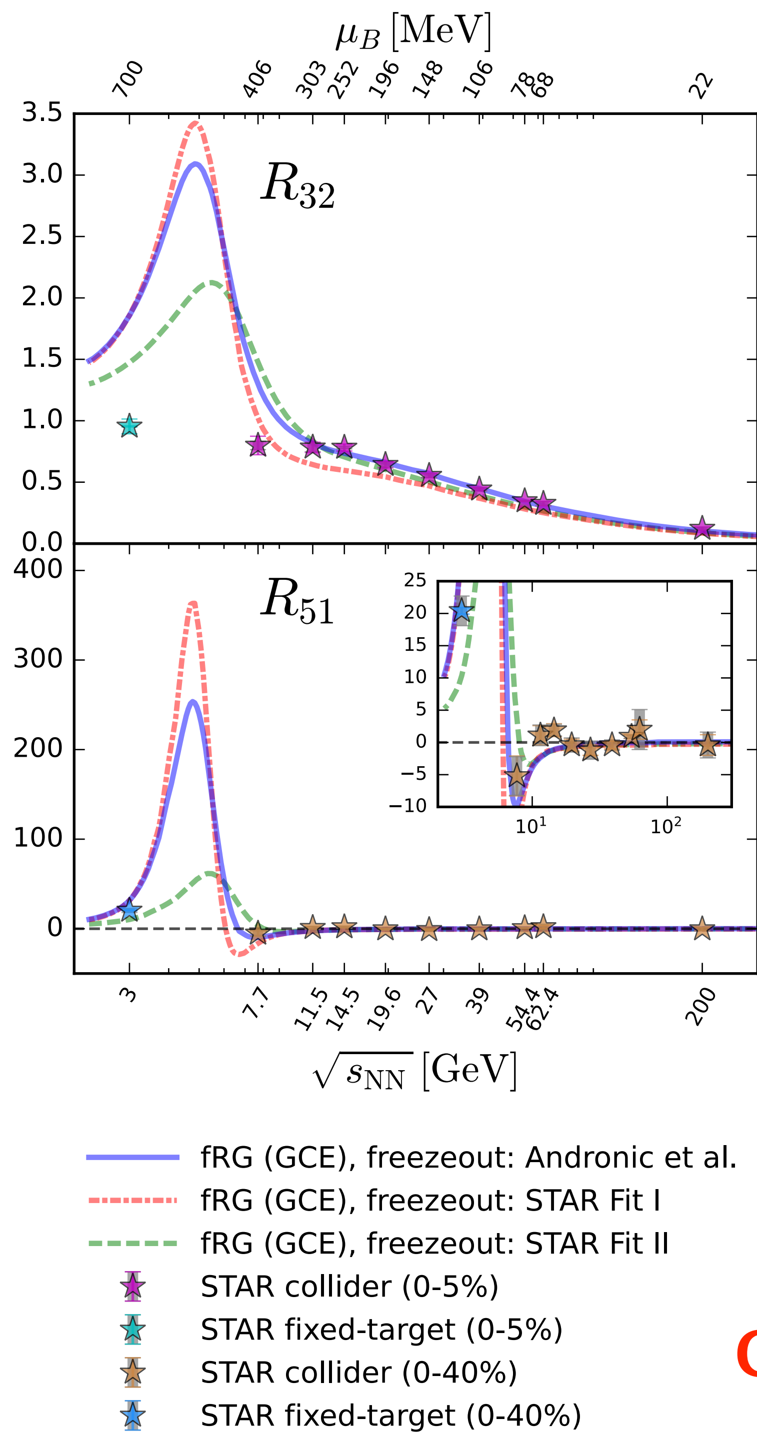

STAR: Adam *et al.* (STAR), *PRL* 126 (2021) 092301; Abdallah *et al.* (STAR), *PRL* 128 (2022) 202303; Aboona *et al.* (STAR), *PRL* 130 (2023) 082301

fRG: WF, Luo, Pawlowski, Rennecke, Yin, *PRD* 111 (2025) L031502, arXiv: 2308.15508

- **Results in fRG are obtained in the QCD-assisted LEFT with a CEP at $(T_{\rm CEP}, \mu_{B_{\rm CEP}}) = (98{,}643)$ MeV.**
- **Peak structure is found in 3 GeV $\lesssim \sqrt{s_{\rm NN}} \lesssim$ 7.7 GeV.**
- **Agreement between the theory and experiment is worsening with $\sqrt{s_{\rm NN}} \lesssim$ 11.5 GeV.**
- **Effects of global baryon number conservation in the regime of low collision energy should be taken into account.**

Caveat:

Fluctuations of baryon number in theory are compared with those of proton number in experiments.

Canonical corrections with SAM

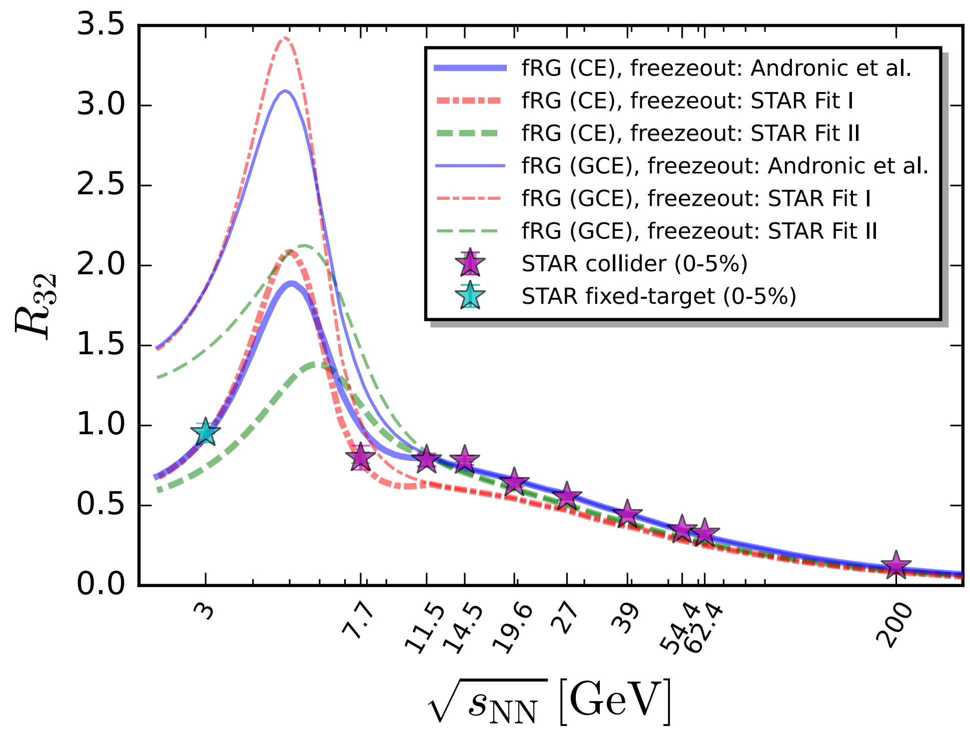

- **Experimental data R_{32} is used to constrain the parameter α in the range $\sqrt{s_{\rm NN}} \lesssim 11.5$ GeV.**
- **We choose the simplest linear dependence**

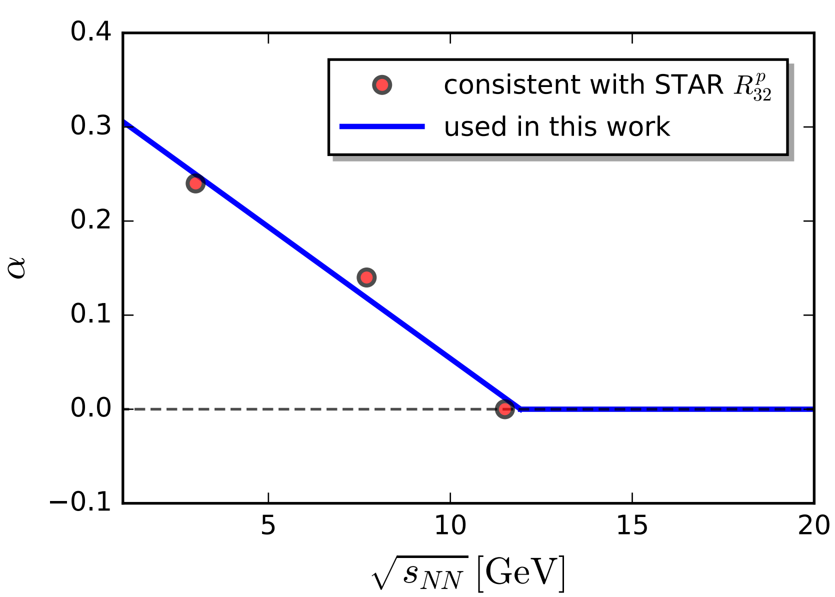

$$\alpha(\bar{s}) = a\left(1 - \sqrt{\bar{s}}\right)\theta\left(1 - \bar{s}\right)$$

$$a = 0.33\,, \qquad \sqrt{\bar{s}} = \frac{\sqrt{s_{\rm NN}}}{11.9\,\text{GeV}}$$

SAM:

- We adopt the subensemble acceptance method (SAM) to take into account the effects of global baryon number conservation:

$$\alpha = \frac{V_1}{V}$$

V_1: the subensemble volume measured in the acceptance window, V: the volume of the whole system.

- fluctuations with canonical corrections are related to grand canonical fluctuations as follows:

$$\bar{R}^B_{21} = \beta R^B_{21}, \qquad \bar{R}^B_{32} = (1-2\alpha)R^B_{32},$$

$$\bar{R}^B_{42} = (1-3\alpha\beta)R^B_{42} - 3\alpha\beta(R^B_{32})^2$$

$$\beta = 1 - \alpha$$

SAM: Vovchenko, Savchuk, Poberezhnyuk, Gorenstein, Koch , *PLB* 811 (2020) 135868

Dependence on the location of the CEP

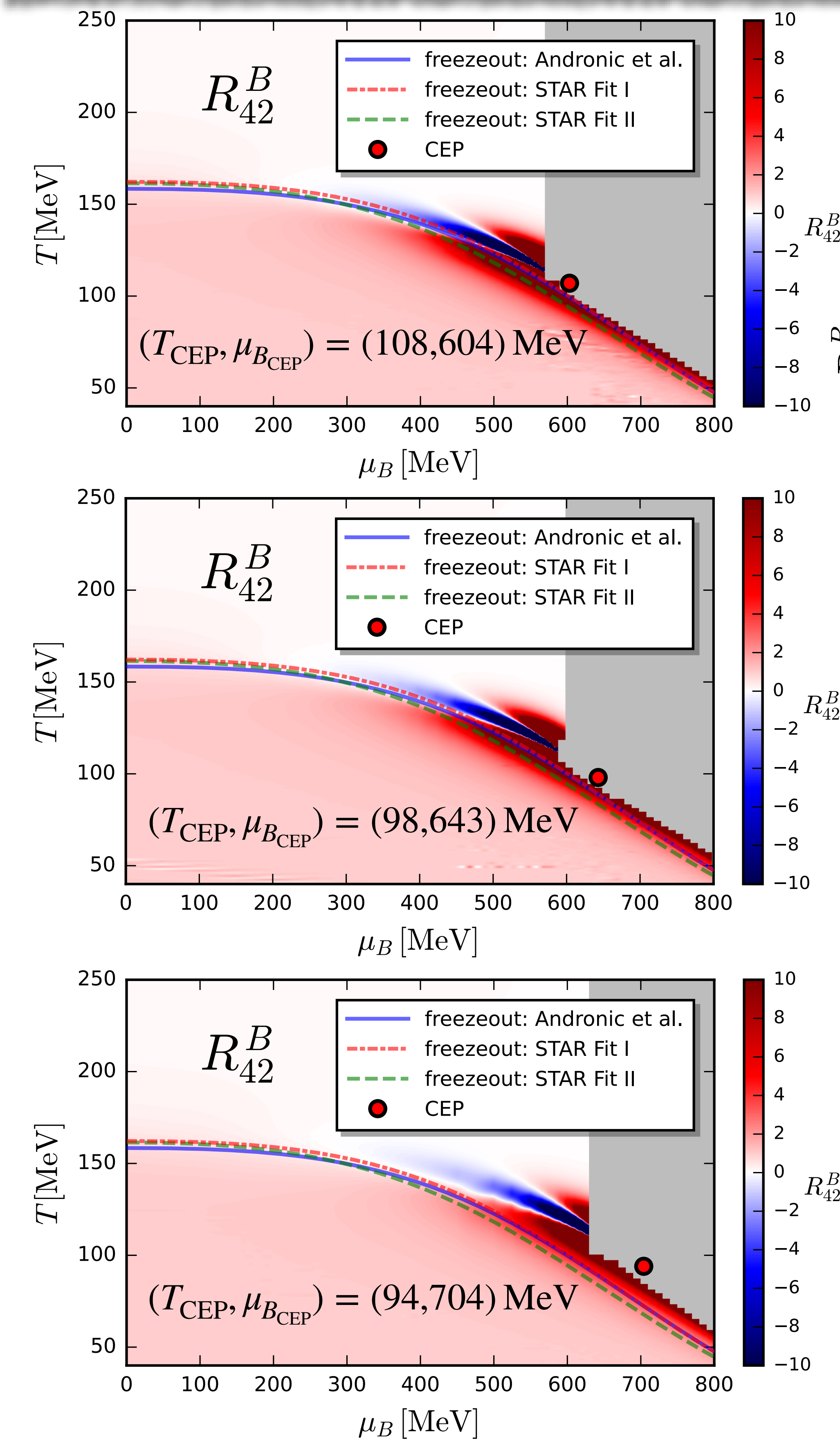

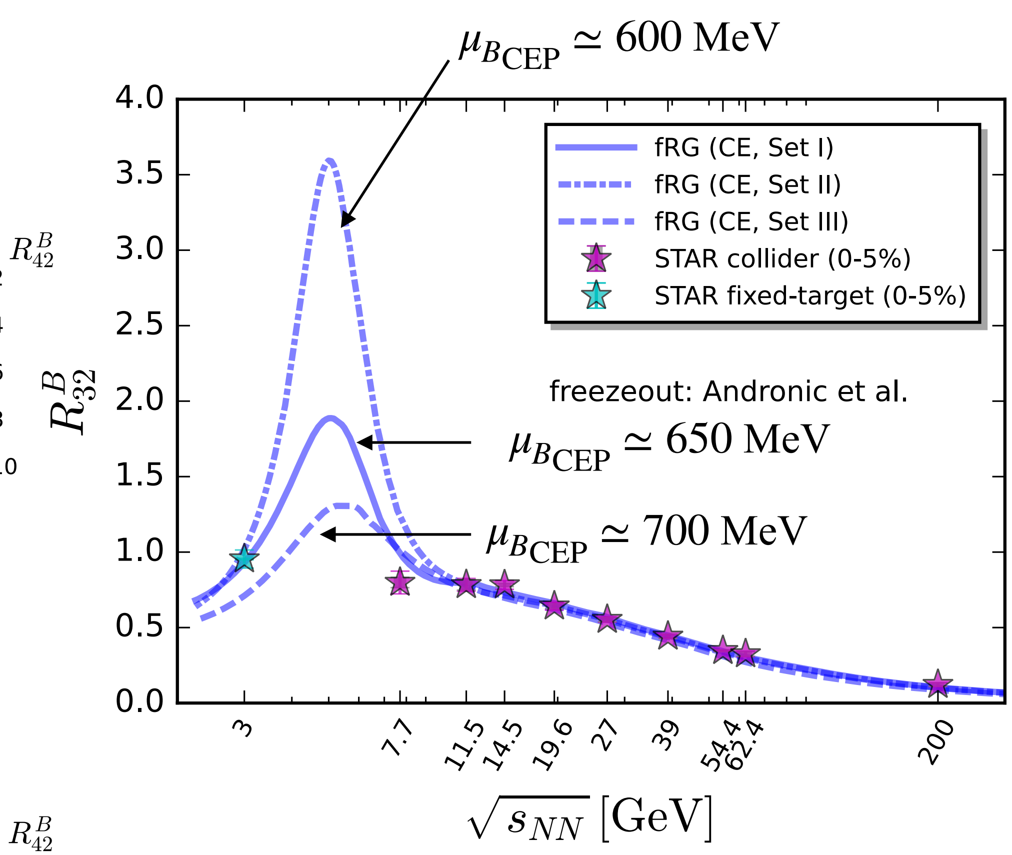

STAR: Adam *et al.* (STAR), *PRL* 126 (2021) 092301

fRG: WF, Luo, Pawlowski, Rennecke, Yin, arXiv: 2308.15508

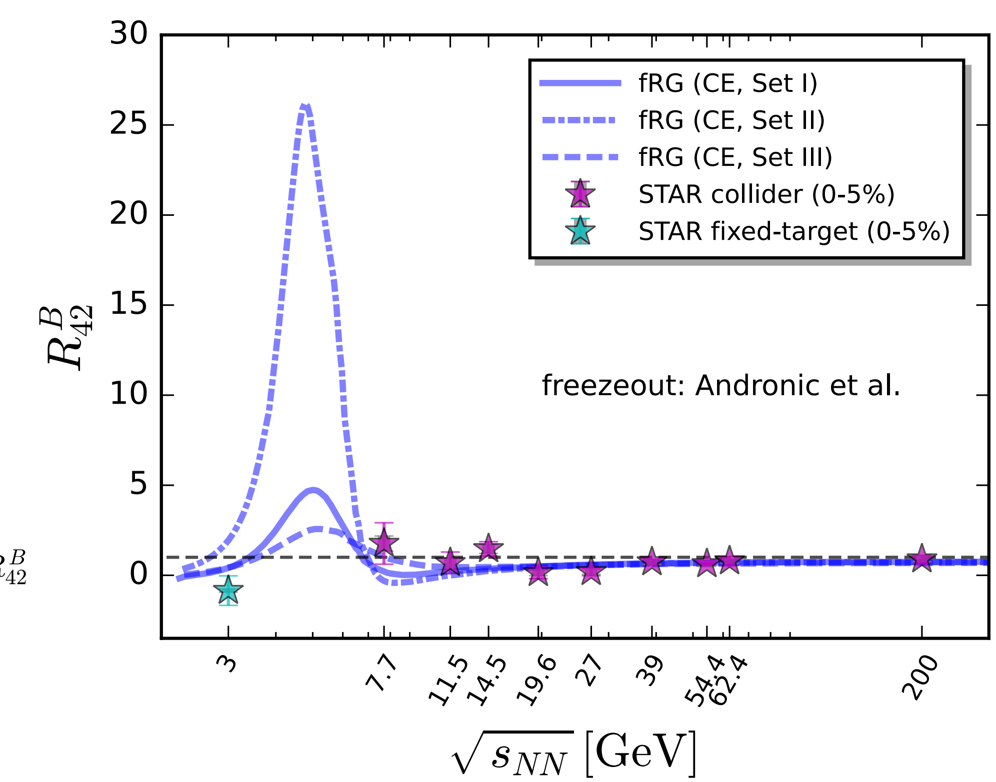

- **Position** of the peak is **insensitive** to the location of CEP.
- **Height** of peak **decreases** as CEP moves towards larger μ_B.

Ripples of the QCD critical point

Position of peak:

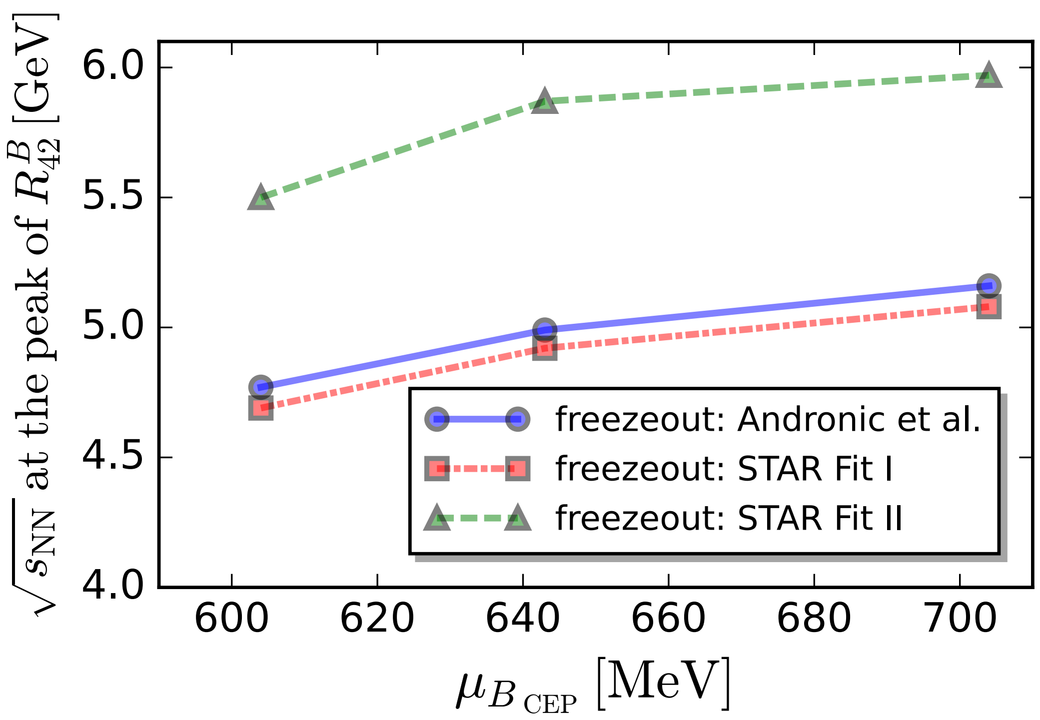

Height of peak:

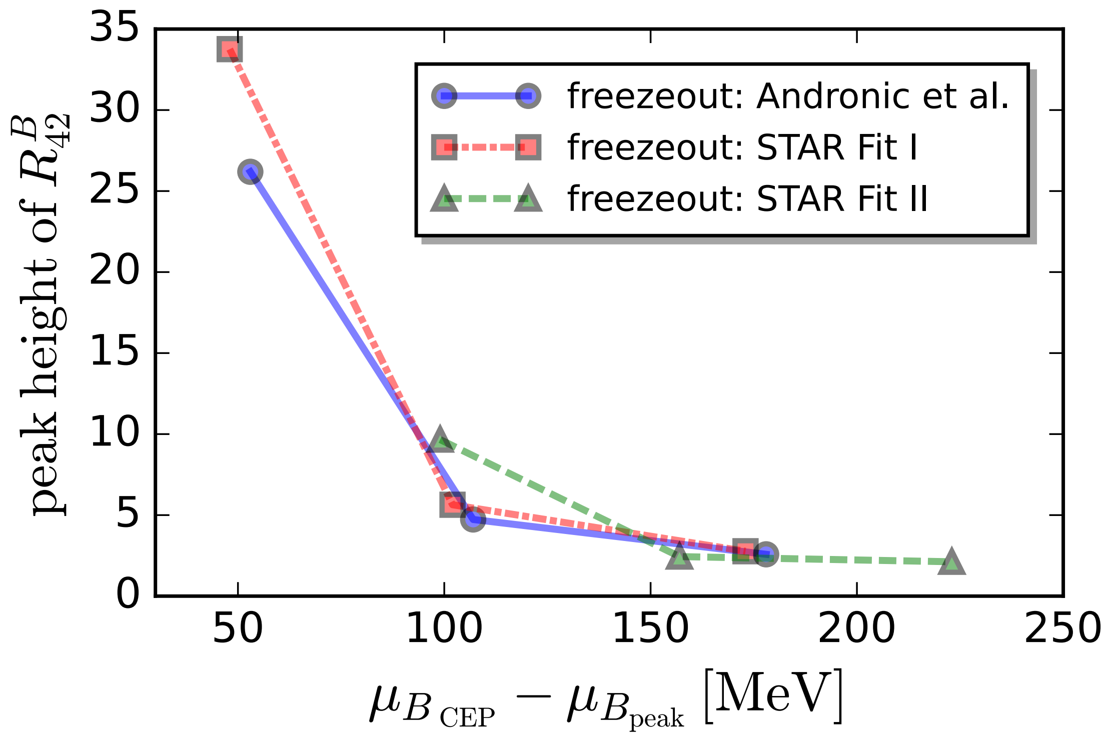

fRG: WF, Luo, Pawlowski, Rennecke, Yin, arXiv: 2308.15508

- **Note that the ripples of CEP are far away from the critical region characterized by the universal scaling properties, e.g., the critical slowing down.**
- **But, the information of CEP, such as its location and properties, etc., is still encoded in the ripples.**

Determination of the freeze-out curve

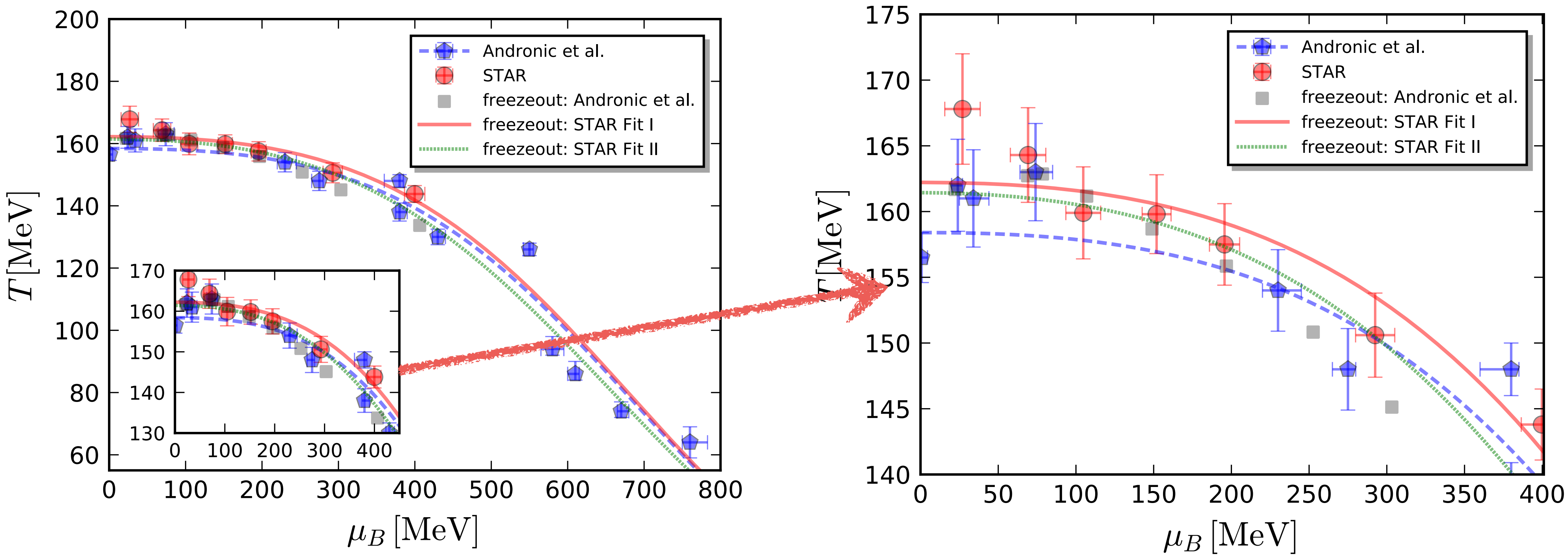

three freeze-out curves

1. freeze-out: Andronic *et al.*

Andronic, Braun-Munzinger, Redlich, *Nature* 561 (2018) 7723, 321

2. freeze-out: STAR Fit I

L. Adamczyk *et al.* (STAR), *PRC* 96 (2017), 044904

$$\mu_{B_{\rm CF}} = \frac{a}{1 + 0.288\sqrt{s_{\rm NN}}}\,,$$

$$T_{\rm CF} = \frac{T_{\rm CF}^{(0)}}{1 + \exp\left(2.60 - \ln(\sqrt{s_{\rm NN}})/0.45\right)}$$

all data points

3. freeze-out: STAR Fit II

neglecting first two at low μ_B and the last one

- freeze-out curve should not rise with μ_B
- convexity of the freeze-out curve

Factorial cumulants of proton (baryon)

Comparison with non-critical HRG and critical fRG:

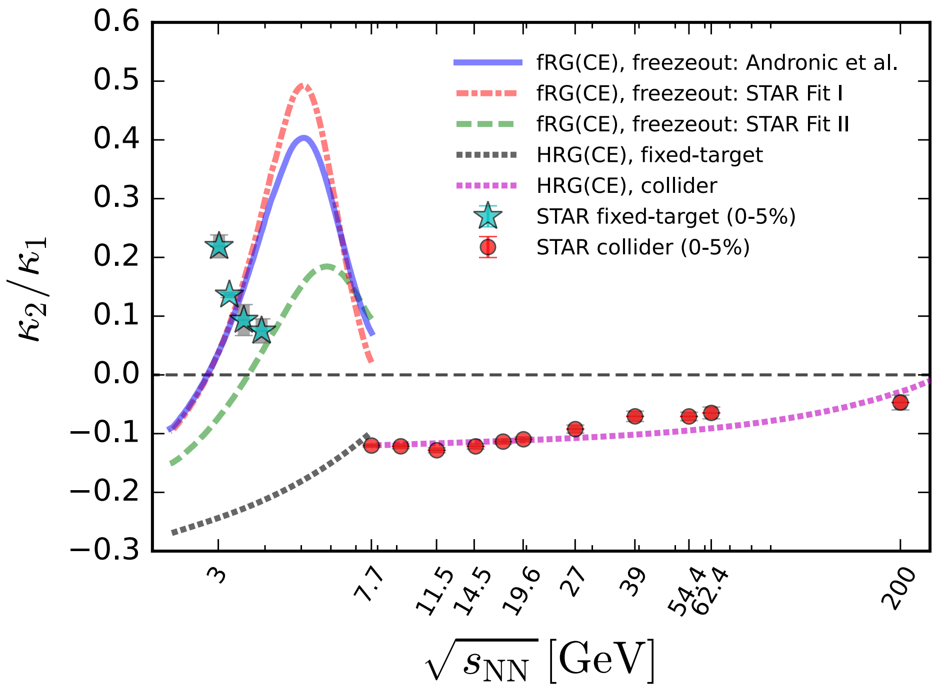

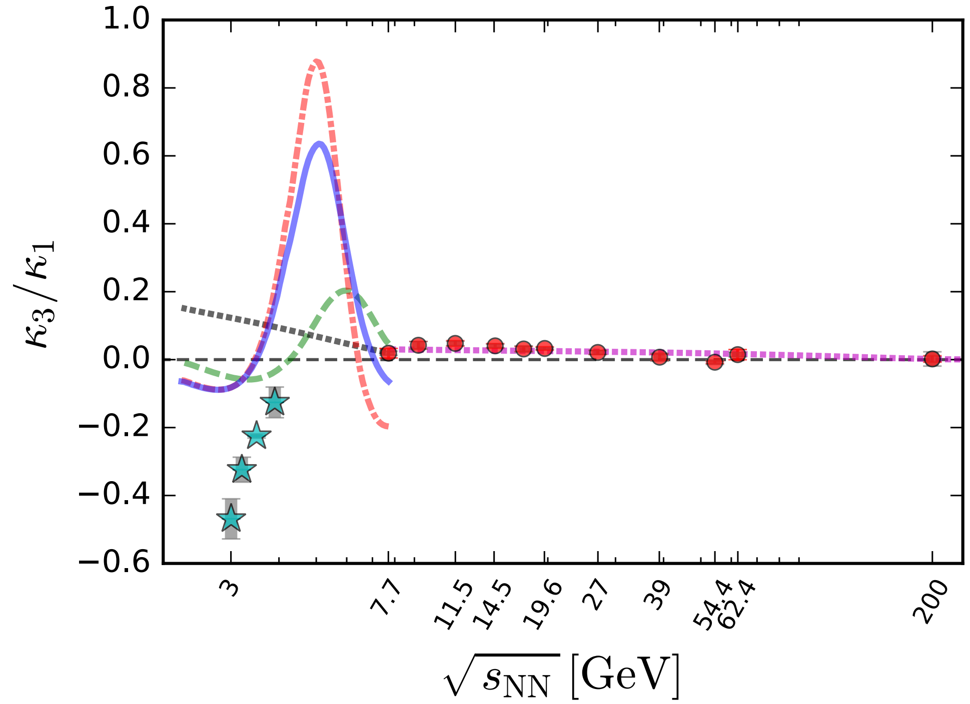

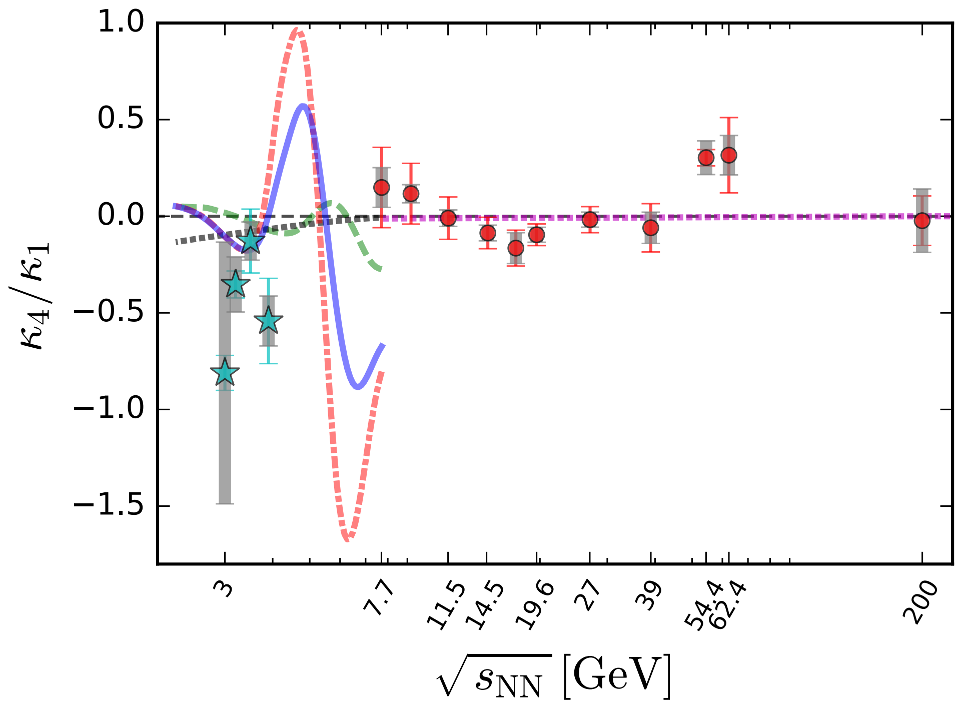

STAR: Quark Matter 2025

STAR: arXiv:2504.00817

fRG and HRG: Zhao, Yin, WF, in preparation

$$\kappa_1 = C_1$$
$$\kappa_2 = -C_1 + C_2$$
$$\kappa_3 = 2C_1 - 3C_2 + C_3$$
$$\kappa_4 = -6C_1 + 11C_2 - 6C_3 + C_4$$

- **In comparison to the non-critical HRG, fRG results with critical fluctuations seem to be better consistent with the data.**

Fierz-complete basis of four-quark interactions

Invariant with the transformation of $SU_V(N_f)$, $U_V(1)$, $SU_A(N_f)$ and $U_A(1)$

$$\mathcal{T}^{(V-A)}_{ijlm}\bar{q}_i q_l \bar{q}_j q_m = (\bar{q}\gamma_\mu T^0 q)^2 - (\bar{q} i\gamma_\mu\gamma_5 T^0 q)^2\,,$$

$$\mathcal{T}^{(V+A)}_{ijlm}\bar{q}_i q_l \bar{q}_j q_m = (\bar{q}\gamma_\mu T^0 q)^2 + (\bar{q} i\gamma_\mu\gamma_5 T^0 q)^2\,,$$

$$\mathcal{T}^{(S-P)+}_{ijlm}\bar{q}_i q_l \bar{q}_j q_m = (\bar{q}\, T^0 q)^2 - (\bar{q}\,\gamma_5 T^0 q)^2 + (\bar{q}\, T^a q)^2 - (\bar{q}\,\gamma_5 T^a q)^2\,,$$

$$\mathcal{T}^{(V-A)^{\mathrm{adj}}}_{ijlm}\bar{q}_i q_l \bar{q}_j q_m = (\bar{q}\gamma_\mu T^0 t^a q)^2 - (\bar{q} i\gamma_\mu\gamma_5 T^0 t^a q)^2\,,$$

Invariant with the transformation of $SU_V(N_f)$, $U_V(1)$, $SU_A(N_f)$, breaking $U_A(1)$

$$\mathcal{T}^{(S+P)-}_{ijlm}\bar{q}_i q_l \bar{q}_j q_m = (\bar{q}\, T^0 q)^2 + (\bar{q}\,\gamma_5 T^0 q)^2 - (\bar{q}\, T^a q)^2 - (\bar{q}\,\gamma_5 T^a q)^2\,,$$

$$\mathcal{T}^{(S+P)^{\mathrm{adj}}_{-}}_{ijlm}\bar{q}_i q_l \bar{q}_j q_m = (\bar{q}\, T^0 t^a q)^2 + (\bar{q}\,\gamma_5 T^0 t^a q)^2 - (\bar{q}\, T^a t^b q)^2 - (\bar{q}\,\gamma_5 T^a t^b q)^2\,,$$

Invariant with the transformation of $SU_V(N_f)$, $U_V(1)$, $U_A(1)$, breaking $SU_A(N_f)$

$$\mathcal{T}^{(S-P)-}_{ijlm}\bar{q}_i q_l \bar{q}_j q_m = (\bar{q}\, T^0 q)^2 - (\bar{q}\,\gamma_5 T^0 q)^2 - (\bar{q}\, T^a q)^2 + (\bar{q}\,\gamma_5 T^a q)^2\,,$$

$$\mathcal{T}^{(S-P)^{\mathrm{adj}}_{-}}_{ijlm}\bar{q}_i q_l \bar{q}_j q_m = (\bar{q}\, T^0 t^a q)^2 - (\bar{q}\,\gamma_5 T^0 t^a q)^2 - (\bar{q}\, T^a t^b q)^2 + (\bar{q}\,\gamma_5 T^a t^b q)^2\,.$$

Invariant with the transformation of $SU_V(N_f)$, $U_V(1)$, breaking $SU_A(N_f)$, $U_A(1)$

$$\mathcal{T}^{(S+P)+}_{ijlm}\bar{q}_i q_l \bar{q}_j q_m = (\bar{q}\, T^0 q)^2 + (\bar{q}\,\gamma_5 T^0 q)^2 + (\bar{q}\, T^a q)^2 + (\bar{q}\,\gamma_5 T^a q)^2\,,$$

$$\mathcal{T}^{(S+P)^{\mathrm{adj}}_{+}}_{ijlm}\bar{q}_i q_l \bar{q}_j q_m = (\bar{q}\, T^0 t^a q)^2 + (\bar{q}\,\gamma_5 T^0 t^a q)^2 + (\bar{q}\, T^a t^b q)^2 + (\bar{q}\,\gamma_5 T^a t^b q)^2\,.$$

Functional renormalization group

Functional integral with an IR regulator

$$Z_k[J] = \int (\mathscr{D}\hat{\Phi}) \exp\left\{ -S[\hat{\Phi}] - \Delta S_k[\hat{\Phi}] + J^a \hat{\Phi}_a \right\}$$

$$W_k[J] = \ln Z_k[J]$$

regulator:

$$\Delta S_k[\varphi] = \frac{1}{2} \int \frac{d^4 q}{(2\pi)^4} \varphi(-q) R_k(q) \varphi(q)$$

flow of the Schwinger function:

$$\partial_t W_k[J] = -\frac{1}{2} \mathrm{STr}\left[\left(\partial_t R_k \right) G_k \right] - \frac{1}{2} \Phi_a \partial_t R_k^{ab} \Phi_b$$

Legendre transformation:

$$\Gamma_k[\Phi] = -W_k[J] + J^a \Phi_a - \Delta S_k[\Phi]$$

flow of the effective action:

$$\partial_t \Gamma_k[\Phi] = \frac{1}{2} \mathrm{STr}\left[\left(\partial_t R_k \right) G_k \right] = \frac{1}{2}$$ 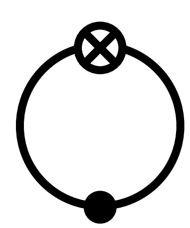

Wetterich formula

C. Wetterich, *PLB*, 301 (1993) 90

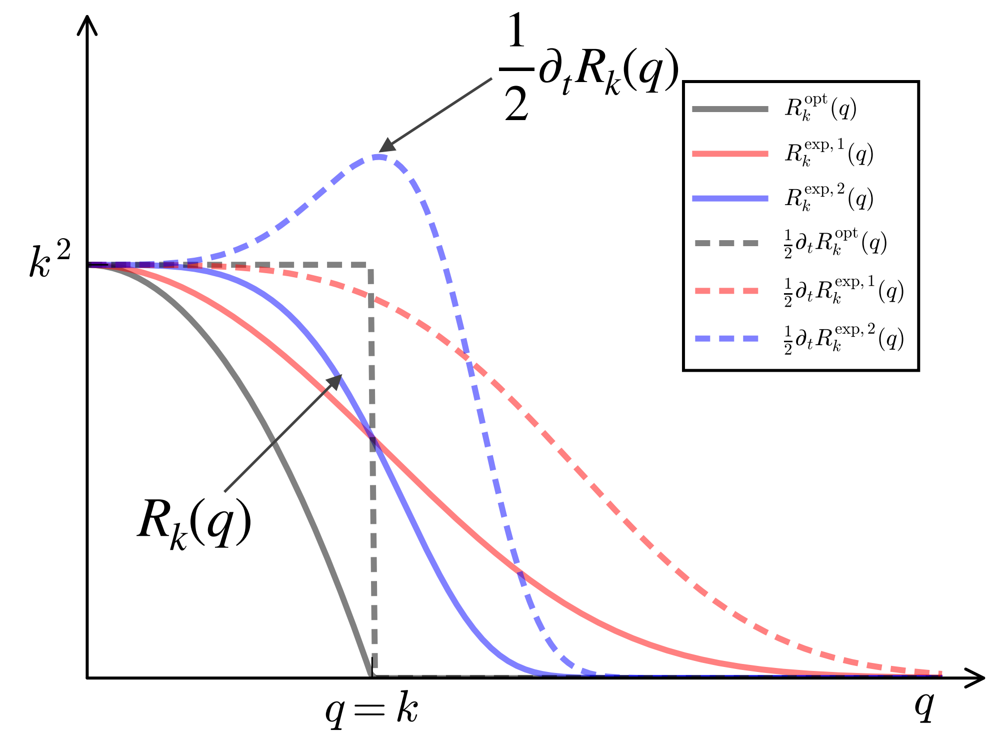

$$G_{k,ab} = \gamma^c{}_a \left(\Gamma_k^{(2)}[\Phi] + \Delta S_k^{(2)}[\Phi] \right)^{-1}_{cb},$$

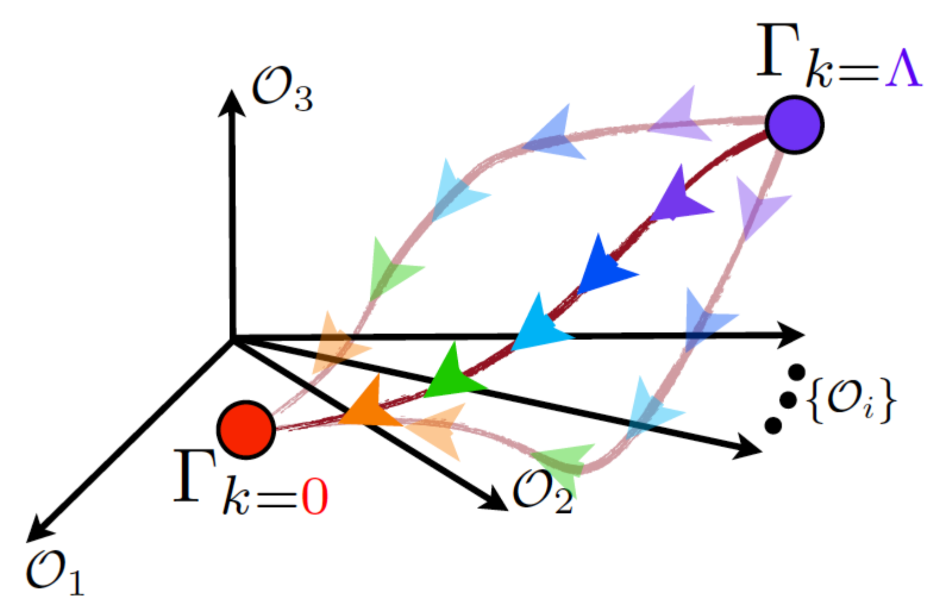

Review: WF, *CTP* 74 (2022) 097304, arXiv: 2205.00468 [hep-ph]